AD/A-004 320

MEASUREMENT OF BALLISTIC IMPACT FLASH

John W. Mansur

Air Force Institute of Technology
Wright-Patterson Air Force Base, Ohio

October 1974

Best
Available
Copy

Best Available Copy

REPORT DOCUMENTATION PAGE

1. REPORT NUMBER	2. GOVT ACCESSION NO.	3. RECIPIENT'S CATALOG NUMBER
GAE/MC/74-29		AD/A-004330

4. TITLE (and Subtitle)
MEASUREMENT OF BALLISTIC IMPACT FLASH

5. TYPE OF REPORT & PERIOD COVERED
MS Thesis

6. PERFORMING ORG. REPORT NUMBER

7. AUTHOR(s)
John W. Mansur
Major, USAF

8. CONTRACT OR GRANT NUMBER(s)

9. PERFORMING ORGANIZATION NAME AND ADDRESS
Air Force Institute of Technology
Wright-Patterson AFB, Ohio 45433

10. PROGRAM ELEMENT, PROJECT, TASK AREA & WORK UNIT NUMBERS

11. CONTROLLING OFFICE NAME AND ADDRESS
Air Force Flight Dynamics Laboratory
Wright-Patterson AFB, Ohio 45433

12. REPORT DATE
October 1974

13. NUMBER OF PAGES
60

14. MONITORING AGENCY NAME & ADDRESS(if different from Controlling Office)

15. SECURITY CLASS. (of this report)
UNCLASSIFIED

15a. DECLASSIFICATION DOWNGRADING SCHEDULE

16. DISTRIBUTION STATEMENT (of this Report)

Approved for public release; distribution unlimited

17. DISTRIBUTION STATEMENT (of the abstract entered in Block 20, If different from Report)

18. SUPPLEMENTARY NOTES

Approved for public release
IAW AFR 190-17

JERRY C. HIX, Captain, USAF
Director of Information

19. KEY WORDS (Continue on reverse side if necessary and identify by block number)

Ballistic Impact
Impact Flash
High Velocity Impact

PRICES SUBJECT TO CHANGE

20. ABSTRACT (Continue on reverse side if necessary and identify by block number)

The downrange flash resulting from the perforation of thin aluminum plates by high velocity steel spheres was investigated to determine how the flash scales with changes in projectile velocity. It was found that two distinct flash intensity maximums occur; one approximately 10 microseconds after penetration, the second some 30 to 60 microseconds later. For a given size sphere, the spectral irradiance of these two flashes and the energy of the flash scale as approximately the fourth power of the velocity. Coating the impact side of the target with epoxy based aircraft paint or a 0.002 inch layer of aircraft ...

DD FORM 1473 1 JAN 73

UNCLASSIFIED
SECURITY CLASSIFICATION OF THIS PAGE (When Data Entered)

Block 20

cell sealant reduced the flash by factors of 5 to 300, depending on the wave-length examined. The first flash spectral irradiance was compared to a black-body temperature curve. The flash was found to radiate as a blackbody source with temperatures increasing from $3000^\circ K$ at 3000 fps projectile velocity to $3200^\circ K$ at 400 fps and 5000 fps.

MEASUREMENT OF BALLISTIC

IMPACT FLASH

THESIS·

Presented to the Faculty of the School of Engineering

of the Air Force Institute of Technology

Air University

in Partial Fulfillment of the

Requirements for the Degree of

Master of Science

by

John W. Mansur, B.S.A.E.
Major   USAF

Graduate-Air Weapons

September 1974

i.h

Preface

This report is the result of my attempt to expand the knowledge available in the area of Ballistic Impact Flash. My principle concern has been determining how the flash scales with changing projectile velocity.

Contents

List of Figures

List of Tables

Abstract

The downrange flash resulting from the perforation of thin alumirum plates by high velocity steel spheres was investigated to determine how the flash scales with changes in projectile velocity. It was found that two distinct flash intensity maximums occur; one approximately 10 microseconds after penetration, the second some 30 to 80 microseconds later. For a given size sphere, both the spectral irradiance of these two flashes and the energy of the flash scale as approximately the fourth power of the velocity. Coating the impact side of the target with epoxy based aircraft paint or a 0.002 inch layer of aircraft fuel cell sealant reduced the flash by factors or 5 to 300, depending on the wavelength examined. The first flash spectral irradiance was compared to a blackbody temperature curve. The flash was found to radiate as a blackbody source, with temperatures increasing from $3000^{\circ}K$ at 3000 fps projectile velocity to $3200^{\circ}K$ at 4000 fps and 5000 fps.

I. Introduction

Throughout modern history, a primary aspect of warfare has been the penetration of metal sheets or plates by high velocity projectiles. Research in this area has traditionally stopped when hostilities cease. As a result, on. serious engineering problem in the area of weapon system design has been the lack of knowledge concerning penetration mechanics. A new area of investigation evolved in the past decade with the advent of space travel. A major concern was the threat to space vehicles from hyper-velocity micrometeorites. A flurry of private and government research in this area began in about 1960, but gradually came to a near stop in 1969, when actual space flights showed the threat to be less than had been feared. While a sizeable amount of data was obtained during this period, it was primarily concerned with projectile velocities of 15,000 foot per second or higher, and projectile sizes of one millimeter diameter or less. A serious lack of information still exists for shrapnel sized projectiles with velocities of 3000 fps to 10,000 fps; the threat that modern day air weapon systems face.

To date, there have been many theories put forward to empirically characterize the penetration and deformation of plates by high velocity projectiles. Although many shots have been fired under carefully controlled conditions in the evolution of these theories, no completely satisfactory model of the penetration has been developed. One of the least understood areas is the flash of light resulting from high velocity impact. This flash is known to be a high temperature phenomena and a major area of concern is the possibility of a fuel tank, hydraulic reservoir, or other explosive componer' of an aircraft being hit by a

1

very high velocity fragment. Until recently, with the exception of space vehicles, only fragments in the range of 5000 fps or less were encountered. Now, however, with aircraft reaching velocities in the range of 3000 fps, and large surface-to-air missiles projecting fragments at 8000 fps to 12,000 fps, impact velocities of 10,000 fps to 15,000 fps might be encountered. Temperatures of $4000^{\circ}K$ and a flash 14 inches long have been reported (Ref 1) from a .50 caliber projectile impacting a thin aluminum sheet at 4000 fps.

The object of this study is to provide further insight into the mechanism of impact flash, specifically to investigate how the flash scales as projectile size and velocity change, and to evaluate the effect on the flash caused by coating the target with various materials.

Background

As a starting point, I will give a summary of the more significant results published relating to this topic.

In 1952, R. L. Kahler (Ref 12) observed that an inert atmosphere reduced the flash, while a pure oxygen atmosphere greatly enhanced the flash. He also noted that if the upstream side of the target was coated with a very thin layer of rubber, the flash was significantly reduced. With his instrumentation, however, he was unable to quantitatively measure this reduction. In 1955, W. T. Thompson (Ref 22), in a report on armor penetration, proposed that the target-projectile interface was molten. In 1957, P. E. Tucker, et. al. (Ref 23), in a study of high speed pellets, observed that a high velocity projectile leaves an ionized, luminous trail, and the relative ionization and luminous intensity increase rapidly with velocity. They also noted that the light occurs prior to the ionization. In 1960, the shift in emphasis to space applications

2

began. D. D. Keough (Ref 13), in 1960, used a photo-multiplier system to measure the intensity of the radiant energy produced by micro-particles at hyper-velocities (16,000 fps) impacting thin metal sheets. His target was in a vacuum chamber, and his results were obtained for various chamber pressures. He reported that the total radiant energy amplitude was not a function of chamber pressure. He suggested that the impact flash mechanism could be modeled as a jet, similar to the jet produced by a shaped charge. A. P. Caron (Ref 6), in 1965 conducted a series of experiments in which aluminum sheets containing oxygen at one atmosphere pressure were impacted by particles traveling in excess of 15,000 fps. He observed that a violent detonation occurred 40 micro-seconds after impact. He suggested that a pyrophoric oxidation reaction of the projectile and target material with gaseous oxygen was the cause of the luminosity. In 1966, J. F. Friichtenicht (Ref 10) proposed that first light is a vapor cloud with plasma-like characteristics including self-luminosity due to the excitation of neutral gas atoms. He observed that the light source appeared to be first, blackbody emission from heated material, and second, radiation from excited atoms in the vapor cloud. In 1967, W. H. Friend, et. al. (Ref 9) observed that for a 12.7 mm projectile fired at 15,000 fps, the intensity maximum occurred 150-200 microseconds after first light was observed, and that after the maximum was reached, the intensity decayed exponentially to zero. They concluded that the exponential decay implied that chemical reactions were not taking place to an appreciable extent, since apparently insufficient heat was being given off to maintain the high intensity. Also, the hot luminous products should take a finite time to cool down, and these processes would be expected to occur in an exponential fashion. Also in 1967,

J. '. Kottensette and E. Wittrock (Ref 14) observed that while the
intensity of the flash is dependent on impact velocity, the light is
spectrally characteristic of the target-projectile materials, and this
spectral characteristic is independent of impact velocity. They also
suggested that first light is generated by transfer of projectile energy
to the target surface before coupling of energy to the crystalline struc-
ture of the target begins. In 1968, B. Jean, et. al. (f 11), following
Keough's lead, mathematically modeled the impact flash as a jet similar
to the jet produced by a shaped charge detonation. Their experimental
and theoretical values were in fairly good agreement. In their experi-
mental work, they compared the flash obtained by impacting projectiles of
various shapes, and observed that spheres and other solid projectiles of
equal mass and like material produce approximately equal radiant energy.
In 1969, J. B. Abernathy (Ref i:32) impacted cylindrical projectiles on
thin aluminum sheets at velocities in the range of 5000 fps. He observed
that the dimensions of the flash were approximately 14 inches long and 5
inches in diameter at the center (See Figure 12). The temperature of the
flash was found to be between 3400°K and 4100°K, and the flash lasted
approximately 3 to 5 milliseconds.

II. Physical Model

The overall physical model of the flash can be divided into four phases. Upon impact, as energy is transferred to the target, first light occurs in what I will call the plasma phase. Material is then removed from the target in the rupture phase. Next, because of their high velocities, the ejected particles are heated and their surface begins to melt and flow during the ablation phase. Finally, the exposed surface area and oxygen from the atmosphere combine chemically giving the burning phase.

Plasma Phase

Abernathy (Ref 1:29), observing target rear surface flash, noted that there are two flash intensity maxima. One occurs simultaneously with the projectile emerging from the rear of the target, and the second some 40-75 microseconds later. This was also verified during the course of this investigation. From Reference 2, it is seen that for high velocity (4000-8000 fps) steel on aluminum impact, pressures in the target are in the .2 to .4 megabar range, and from Reference 16, peak shock temperatures occur that are in excess of $1000^{\circ}K$. This high temperature, high pressure, nigh energy state produces the first-light, plasma-like cloud proposed in Reference 10:1. This might also explain why several researchers have noted that first light or peak amplitude seems to be independent of pressure or atmosphere.

Rupture Phase

There are many references (Ref 15, Ref 19) presenting careful documentation for increased temperatures in the particles being ejected

by ballistic impact. It is clear that these ejecta have a high internal energy, and thus a high temperature, after being torn from the target plate.

Ablation Phase

As the high velocity particles are decelerated by drag, the air friction creates enough heating to cause the surface to melt and be swept off in the form of tiny droplets as discussed by Kottenstette in Reference 14. This continually exposes new surface area and also provides smaller particles or droplets for the burning phase. This phase and the burning phase would be greatly affected by the atmosphere around the target, as was reported by Kahler (Ref 12).

Burning Phase

As the droplets produced during the ablation phase continue to decelerate due to striking air molecules, they gain sufficient thermal energy to reach the necessary temperature to combine with oxygen to produce light (Ref 4:25). The time required to gain this additional energy is thought to account for the time lapse between first light and the second intensity maximum. Boice in Reference 4 presents a comprehensive discussion of the rupture, ablation, and burning phases.

An additional factor adding thermal energy to the ejecta is the shock heating of the air that the ejecta travels through. An approximate temperature behind the shock wave can be calculated using the Rankine-Hugoniot jump conditions across a plane steady shock (Ref 23:22). Let P = pressure, ρ = density, E = energy, U = particle velocity, D = shock velocity, and the subscripts o and F indicate before and after shock respectively. Then, the equation of conservation of mass,

6

$$P_F(D-U_F) = \rho_O D, \tag{1}$$

the equation of conservation of momentum,

$$P_F = \rho_O D \, U_F, \tag{2}$$

and an energy balance (neglecting heat flow across the shock and heat release or losses)

$$E_F - E_O = \frac{P_F U_F}{\rho_O D} - 1/2 \, U_F^2, \tag{3}$$

combined with an assumption of a perfect gas,

$$P = \rho R T \tag{4}$$

and

$$E = C_V T, \tag{5}$$

give sufficient relationships to solve for the post shock values.

Using (1), (2), (4), and (5) with (3) gives

$$C_V(T_F - T_O) = \left(\frac{P_F + P_O}{2}\right)\left(\frac{1}{\rho_O} - \frac{1}{\rho_F}\right). \tag{6}$$

Further reducing unknowns gives

$$(D-U_F)\left(\frac{C_V U_F}{R} + \frac{U_F}{2} + \frac{P_O}{2\rho_O D}\right) - \frac{D \, U_F}{2} = C_V T_O + \frac{P_O}{2\rho_O} \tag{7}$$

since

$$R = C_V(\gamma-1) \tag{8}$$

where γ is the gas constant.

Equation (7) can be further reduced to

$$(D-U_F)\left(\frac{U_F}{\gamma-1} + \frac{U_F}{2} + \frac{P_O}{2\rho_O D}\right) - \frac{D \, U_F}{2} = \frac{P_O}{\rho_O(\gamma-1)} + \frac{P_O}{2\rho_O} \tag{9}$$

which is an easily solvable quadratic equation.

Typical values for a shot are

$$P_O \quad = \quad 1 \text{ atmosphere} = 2117 \frac{lb}{ft^2}$$

$$\rho_O \quad = \quad .002378 \frac{lb \; sec^2}{ft^4}$$

$$\gamma \quad = \quad 1.4 \text{ for a perfect gas}$$

$$U_O \quad = \quad 0$$

$$V_{IMPACT} \quad = \quad 4360 \text{ fps.}$$

Reference 4 shows that for a steel on aluminum impact of 4360 fps, the aluminum particle velocity in the plate would be 3011 fps. When a plane shock wave arrives at a free surface, which is assumed parallel to the shock front, the shock pressure is reduced to zero by a rarefaction wave from the free surface. The free surface particle velocity, or velocity of the particles departing the back of the target in this case, is the sum of the particle velocity due to the shock wave and the particle velocity due to the rarefaction wave (Ref 20:29). These two velocities are very nearly equal. In this case then, the particle velocity coming off the back of the plate would be twice the value of the particle velocity in the plate, or 6022 fps. Since this would be the same as the air particle velocity immediately behind the plate, $U_F = 6022$ fps.

Using these values in (9) gives $D = 7390$ fps.

Using this in (2) gives $P_F \approx 49.98$ atmospheres, and from (6) $\rho_F = .01285$, and finally $T_F = 2724^O K$, where T_F is the temperature immediately behind the shock wave. Deal, in Reference 1, shows that for this pressure and compression ratio, the use of the perfect gas assumption gives a good approximation to experimental results. The residual temperature, T_R, after the pressure returns to one atmosphere can now be calculated

8

from

$$\left(\frac{T_R}{T_F}\right)^{\gamma} = \left(\frac{P_R}{P_F}\right)^{\gamma-1} \tag{10}$$

Using the above values for T_F, P_F, and γ gives

$$T_R = 896 \,^{\circ}K$$

The volume of air actually being shock heated to this temperature will be relatively small, located immediately downstream of the impact. It will, however, occupy the space that most of the ejecta will travel through. These higher temperatures will increase the thermal energy of the ejecta and will affect the time required to ablate and burn.

III.   Experimental Method

Two sizes of steel spheres were fired from a 50 caliber smooth bore gun through a velocity measuring device and through a 0.0625 inch thick sheet of 2024 T-3 aluminum. A few targets were coated with epoxy based aircraft paint and a few were coated with a 0.002 inch layer of aircraft fuel cell sealant. Front face flash and gun muzzle flash were screened off and the rear face flash was examined by a specially designed spectrometer and a still camera.

Projectiles

Steel spheres were chosen as projectiles to reduce the variables as much as possible. The steel should have a minimum of deformation and chemical reaction with the softer aluminum targets, and the spherical shape eliminates any concern for the position of the projectile at impact. Two sizes were chosen to allow comparison of results for projectiles of different mass and size. The spheres were 0.500 inches in diameter weighing 129.5 grains and 0.343 inches weighing 42.5 grains. The 0.500 inch sphere was crimped directly into the 0.50 caliber casing, while a Lexan sabot was used to hold the 0.343 inch sphere.

The sabot was designed to separate from the projectile upon leaving the gun, and was deflected from the projectile path by a sheet of armor plate having a two inch diameter hole for the projectile to pass through located 15 feet from the gun. The projectile velocities were varied by varying the amount of powder loaded in the cartridge from 80 grains to the maximum capacity of 205 grains.

10

Spectrometer

A spectrometer consisting of three photomultiplier tubes was used to record the downstream flash. Each photomultiplier was equipped with a different narrow band by-pass filter to allow investigation of three distinct areas of the visible and near IR spectrum. The first filter centered at $4008A^{\circ}$ with a bandwidth of 200A; the second centered at $7010A^{\circ}$ with a bandwidth of $200A^{\circ}$; and the third centered at $9025A^{\circ}$ with a bandwidth of $290A^{\circ}$. The output from each of the photomultipliers was the input for a single sweep oscilloscope. The scope sweep rate was adjusted to allow recording of the entire event. The oscilloscope trace was recorded on Polaroid film to allow later examination and measurement. The photomultiplier tubes were calibrated against a standard light source in units of $watts/cm^2$-nanometer. A limitation of this spectrometer is that the photomultiplier tubes are easily saturated. To prevent this, Kodak neutral density filters were used in front of the narrow band by-pass filters. The strength of the filters was increased as the flash intensity increased with increasing projectile velocity. These filters were calibrated against the standard light source to determine the amount of light they passed at the three wavelengths, and this data is presented in Appendix B.

Still Camera

A 4 x 5 speed graphic camera was used to record an image of the total flash. The shutter was opened just prior to the shot, and closed after the shot. The image was recorded on Polaroid film.

IV. Results and Discussion

The downstream flash has two distinct spectral irradiance maxima as shown by the photomultiplier traces in Figure 1.
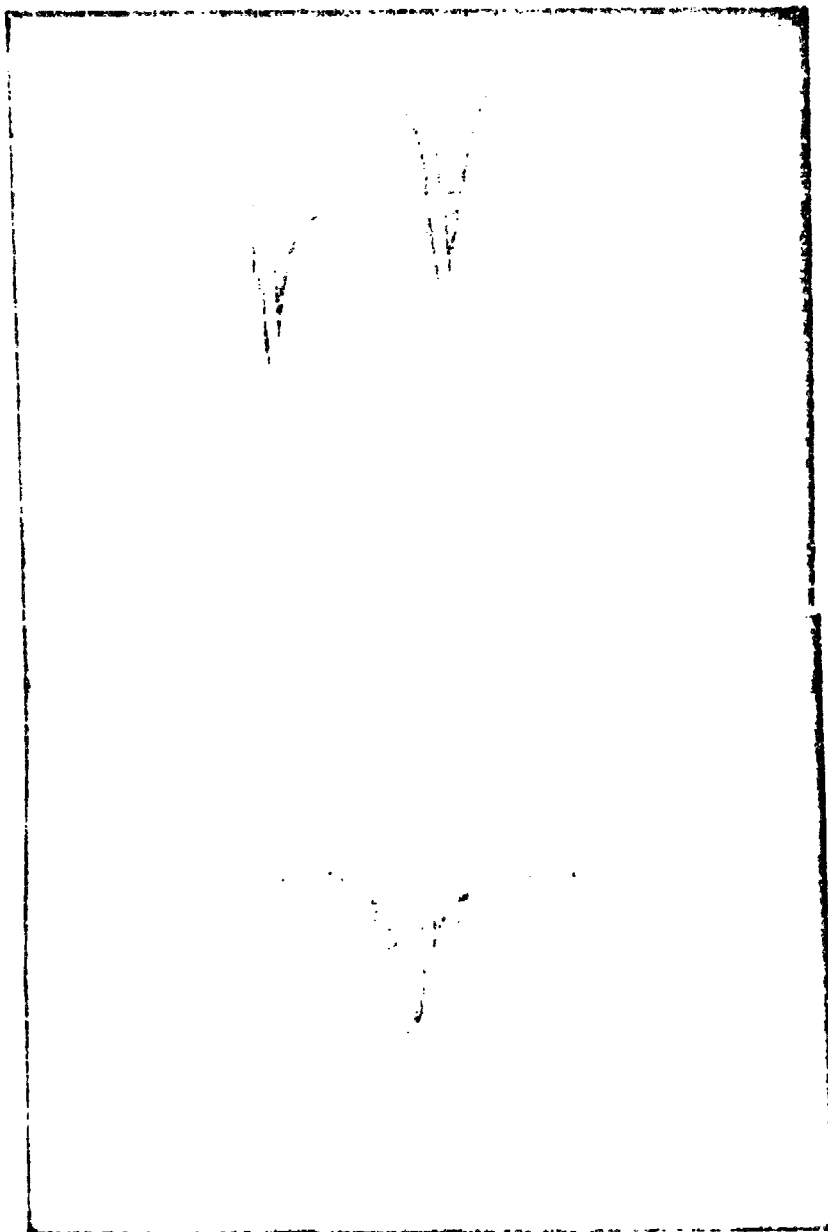

Figure 1. Photomultiplier Traces

This confirms Abernathy's findings in Reference 1:29. In the top

photograph of Figure 1, the upper trace is for the 4008A^o filtered tube,

the lower trace is for the 9025A^o tube. The bottom photograph is for

the 7010A^o tube. All three traces are recorded at a sweep rate of 0.1

millisecond per centimeter, for a 0.500 inch projectile with a velocity

of 3860 fps. The first maximum occurs nearly simultaneously with pene-

tration and is suggested to be front face plasma drawn through the

target in the wake of the projectile. Photographs in Reference 3:7

indicate that this does occur. This flash reaches its peak in approxi-

mately 10 microseconds. The second flash gains in intensity at a slower

rate, reaching its maximum value 30 to 80 microseconds after the onset of

the first flash. After reaching this second maximum, the flash decays in

an exponential fashion to zero. The time required to reach maximum

intensity decreases as wavelength increases, but the duration of the

total flash appears to be independent of wavelength. Tables I, II, and

III list the experimental results by projectile size. Included are

spectral irradiance for first and second maxima and flash energy emitted

in the wavelength bands passed by the narrow band by-pass filters,

obtained by integrating the area under the photomultiplier trace. Values

for the second maxima and for the energy were not obtained for the smal-

ler projectile due to difficulties in measuring these values accurately

from the photomultiplier trace. The results of these tables are plotted

in Figures 2 through 11. Since the experimental values appear to plot

as a straight line on log-log scale paper, a least squares curve fit for

an exponential curve was used to obtain the line drawn on the plots.

This line has an equation of the type

$$X = Kv^n \qquad (11)$$

Table I

Spectral Irradiance of First and Second Flash Maxima from Impact of 0.500 Inch Sphere

Velocity Ft/Sec	First Maximum Spectral Irradiance-Microwatts/cm²-nm			Second Maximum Spectral Irradiance-Microwatts/cm²-nm		
	4008A°	7010A°	9025A°	4008A°	7010A°	9025A°
2194	.00043	.00481	.00847	n	n	n
2290	.00113	.00651	.0113	n	n	n
2658	.001355	.00970	.0211	n	n	n
3077	.0029	.0227	.0423	n	n	.0353
3005	.00347	.0258	.0599	.0069	.0259	.0664
3111	.00455	.0232	.0466	.0114	.0464	n
3172	.00262	.0194	.0353	n	n	.0318
3197	.00231	.0227	.0353	n	n	n
3235	.0050	.0260	.0504	.0059	.0259	n
3330	.00407	.0292	.0635	n	n	n
3386	.00635	.0371	.0790	n	n	.0776
3421	.00407	.0292	.0670	.0168	.0551	.113
3450	.00637	.0388	.0776	.0116	.0712	.106
3489	.00435	.0292	.0705	.0114	.0650	.0664
3514	.0057	.0278	.0597	.0091	.0464	n
3528	.0057	.0278	.0597	n	n	.0597
3539	.00912	.0371	.0790	.0102	.0464	.0860
3554	.00635	.0325	.0730	.0159	.0650	.0860
3605	.00300	.0371	.0790	.0136	.0650	.0776
3642	.00912	.0465	.0730	.0116	.0487	.0847
3643	.00315	.0487	.0938	.0139	.0551	.0847
3673	.00755	.0497	.106	.0148	.0650	.0931
3637	.00912	.0557	.0846	.0148	.0650	.0797
3695	.00300	.0511	.0361	.0171	.0698	n
3725	.00970	.0511	.0790	n	n	
3749	.0091	.0418	.0361			

n - Data Not Obtained

14

Table 1 (Continued)

Spectral Irradiance of First and Second Flash Maxima from Impact of 0.500 Inch Sphere

Velocity Ft/Sec	First Maximum Spectral Irradiance-Microwatts/cm²-nm			Second Maximum Spectral Irradiance-Microwatts/cm²-nm		
	4008A°	7010A°	9025A°	4008A°	7010A°	9025A°
3767	.0102	.0650	.0931	.0228	.0884	.106
3859	.0102	.0557	.0931	.0114	.0603	.0861
3860	.0102	.0511	.107	.0204	.0790	.113
3361	.0114	.0743	.133	.0171	.102	.125
3653	.0114	.0557	.0994	.0132	.0557	.106
3941	.0125	.0552	.113	.0133	.0557	.0931
3959	.0097	.0697	.113	.0114	.0650	.0860
3965	.0137	.0650	.119	.0136	.0744	.113
4167	.0125	.0743	.113	.0182	.0790	.113
4281	.0125	.0743	.133	.0171	.102	.125
4295	.0159	.0743	.133	.0228	.0931	.173
4300	.0142	.0743	.133	n	n	n
4330	.0136	.0782	.133	.0239	.121	.146
4335	.0171	.0929	.146	.0262	.102	.133
4436	.0171	.0827	.159	.0472	.205	.279
4454	.0132	.0921	.172	.0615	.205	.252
4596	.0204	.0931	.211	n	n	n
4770	.0205	.102	.159	n	n	n
4966	.0274	.112	.199	.0500	.167	.239
5014	.0273	.112	.185	.0365	.167	.212
5120	.0295	.130	.212	.0455	.149	.239

n - Data Not Obtained

15

Table II

Flash Energy From Impact of 0.500 Inch Sphere

Velocity Ft/Sec	Total Energy-Ergs/cm^2 -nm		
	4008A°	7010A°	9025A°
3111	.0068	.0318	.0509
3450	.0065	.0362	.0517
3489	.0113	.161	.202
3518	.0080	.171	.224
3528	.0072	.0464	.0825
3603	.0061	.0262	.0465
3642	.0068	.0576	.109
3643	.0058	.089	.151
3678	.0096	.0973	.152
3687	.0073	.0580	.0676
3695	.0076	.0402	.133
3749	.025	.145	.135
3767	.0144	.0697	.102
3859	.0072	.0523	.109
3860	.0175	.0783	.128
3941	.0091	.0625	.133
3959	.0075	.0609	.106
4148	.0111	.0987	.093
4281	.0292	.369	.396
4295	.0425	.185	.398
4330	.0219	.323	.434
4385	.0175	.110	.172
4436	.0335	.336	.638
4454	.0365	.139	.309
4596	.0272	.348	.889
4770	.0182	.210	.273
4966	.03	.162	.221
5014	.073	.509	.825
5120	.0335	.232	.380

Table III

Spectral Irradiance of First Flash Maxima
From Impact of 0.343 Inch Sphere

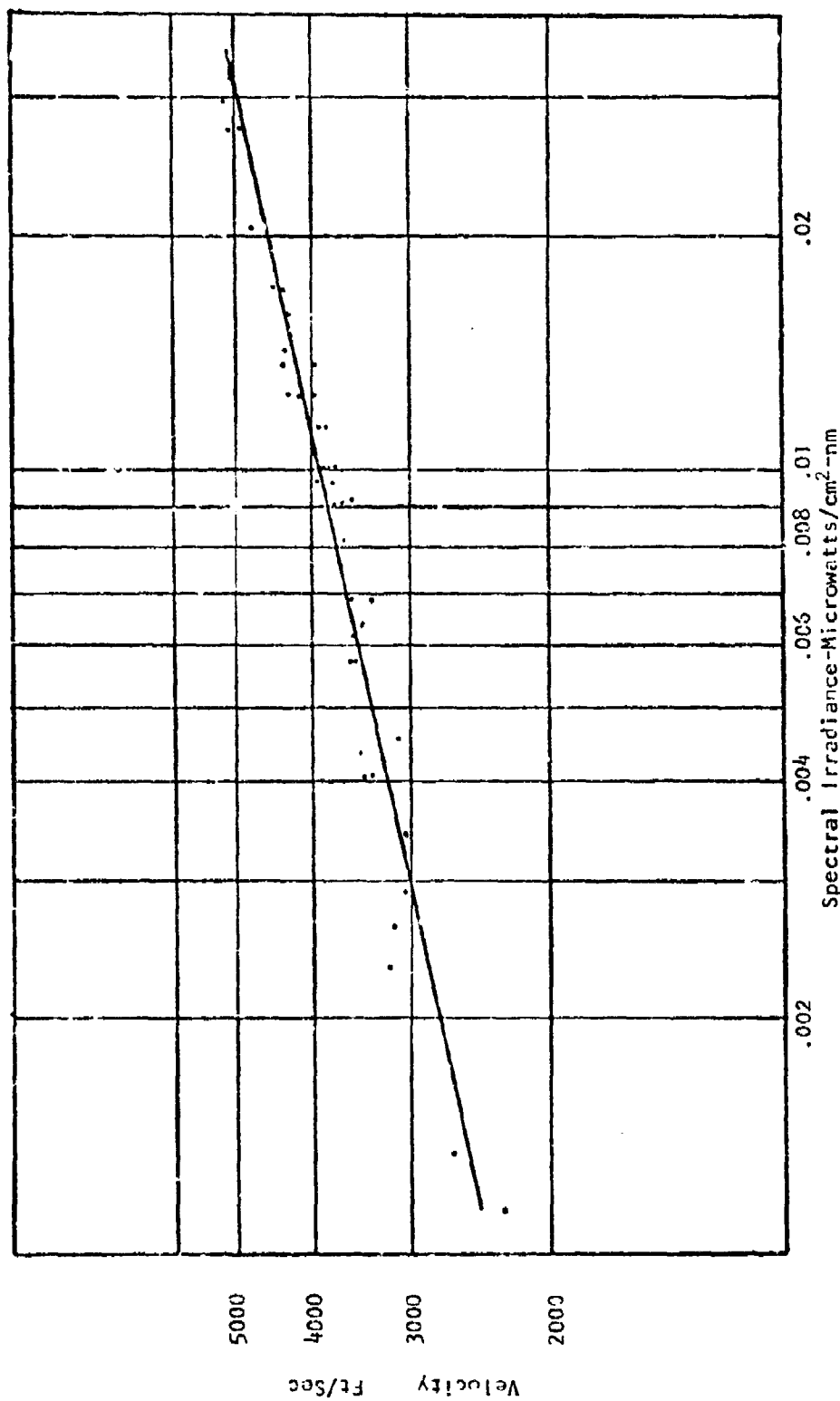| Velocity Ft/Sec	Spectral Irradiance-Microwatts/cm^2-nm		
	4008A$^\circ$	7010A$^\circ$	9025A$^\circ$
3347	.0014	.0113	.0281
3351	.0016	.0138	.0324
3360	.0016	.0122	.0310
3668	.0029	.0161	.0395
3681	.0031	.0210	.0507
3750	.0029	.0227	.0536
3770	.0029	.0210	.0536
3844	.0031	.0227	.0507
3891	.0041	.0227	.0577
3896	.0031	.0237	.0620
3912	.0014	.0357	.0395
3939	.0035	.0227	.0536
3995	.0043	.0227	.0522
4028	.0046	.0275	.0663

Figure 2. 4008A° First Spectral Irradiance Maximum vs Velocity for 0.500 inch Sphere
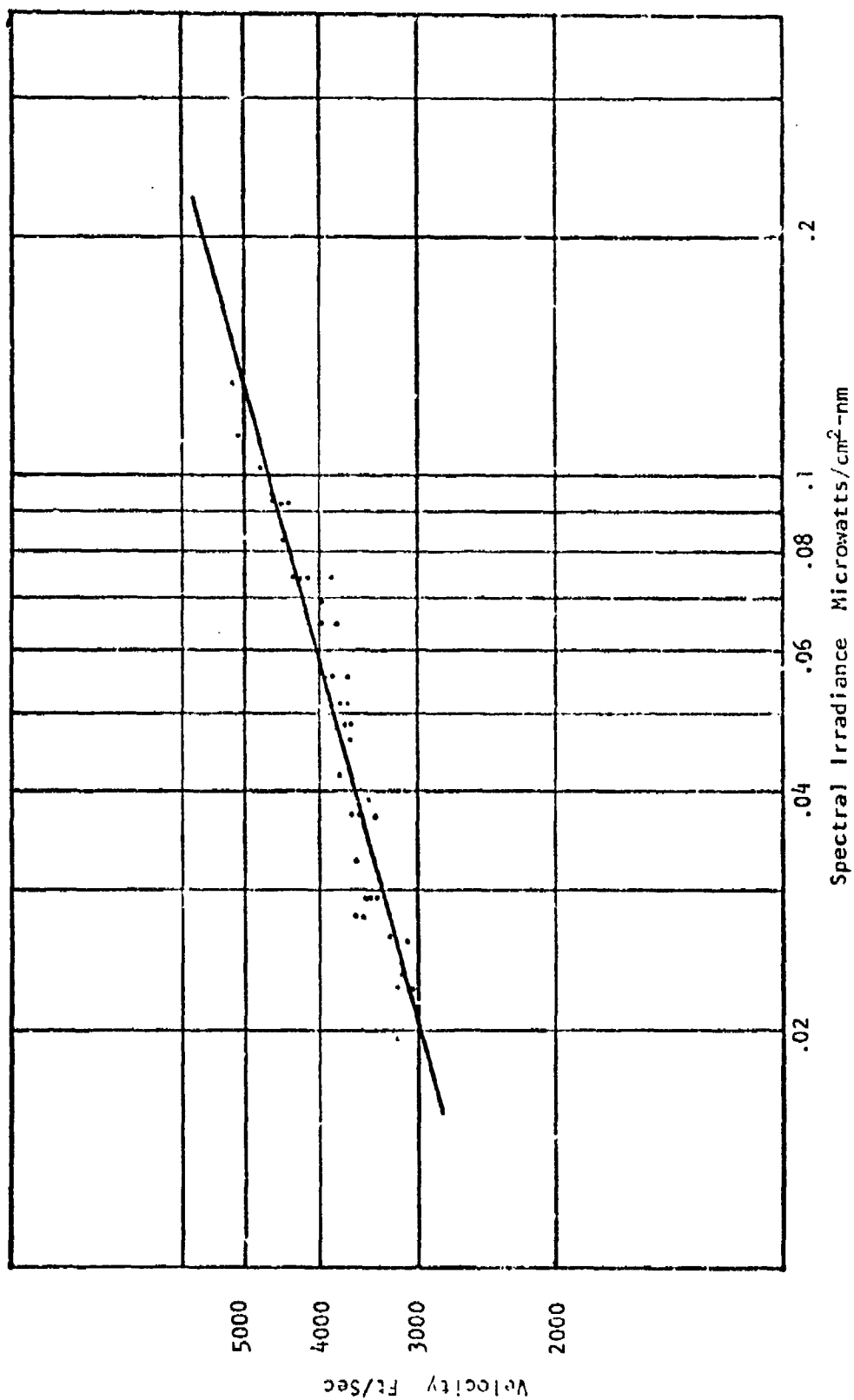
Figure 3. 7010A° First Spectral Irradiance Maximum vs Velocity for 0.500 inch Sphere
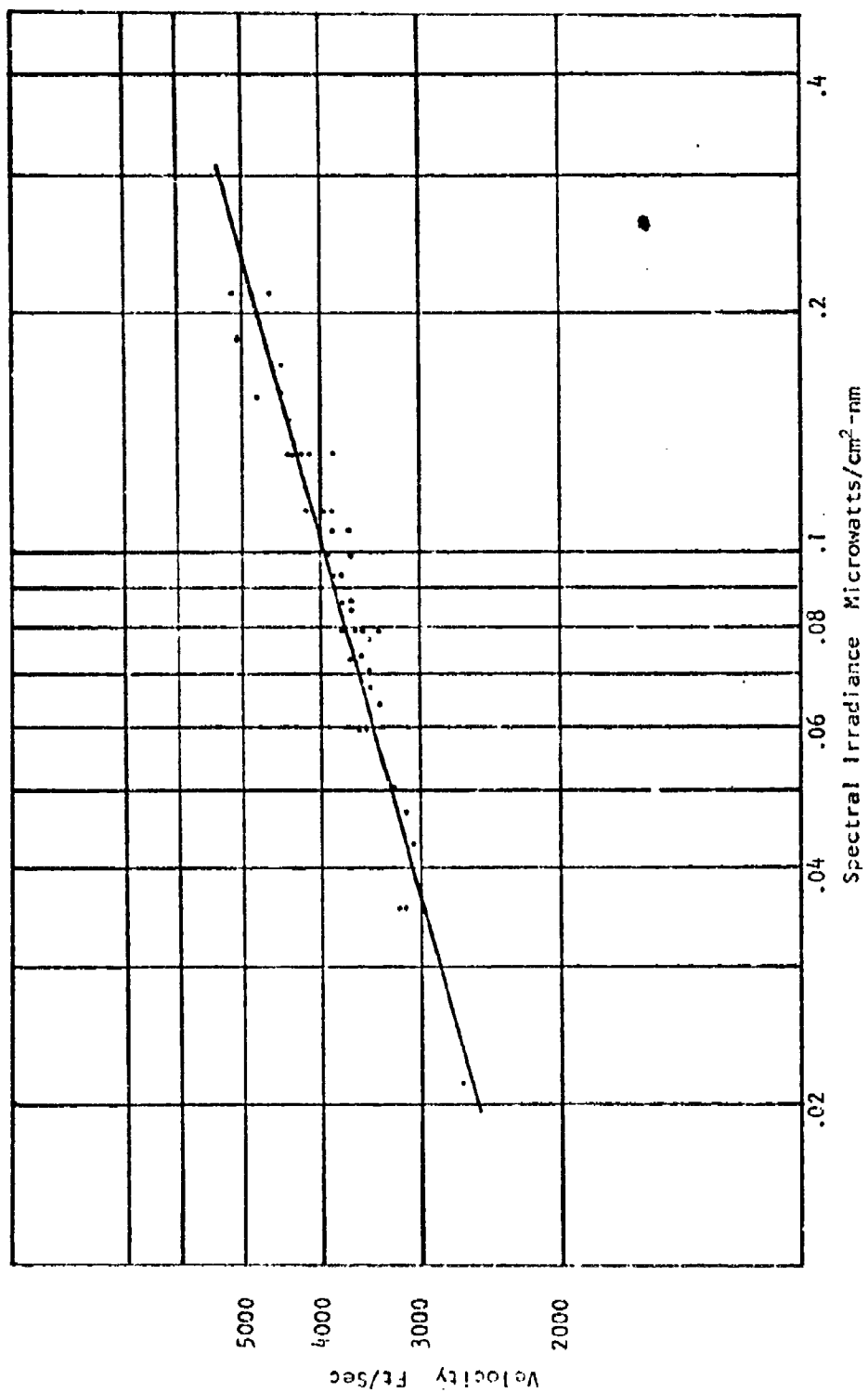
19

Figure 4. 9025A° First Spectral Irradiance Maximum vs Velocity for 0.500 inch Sphere
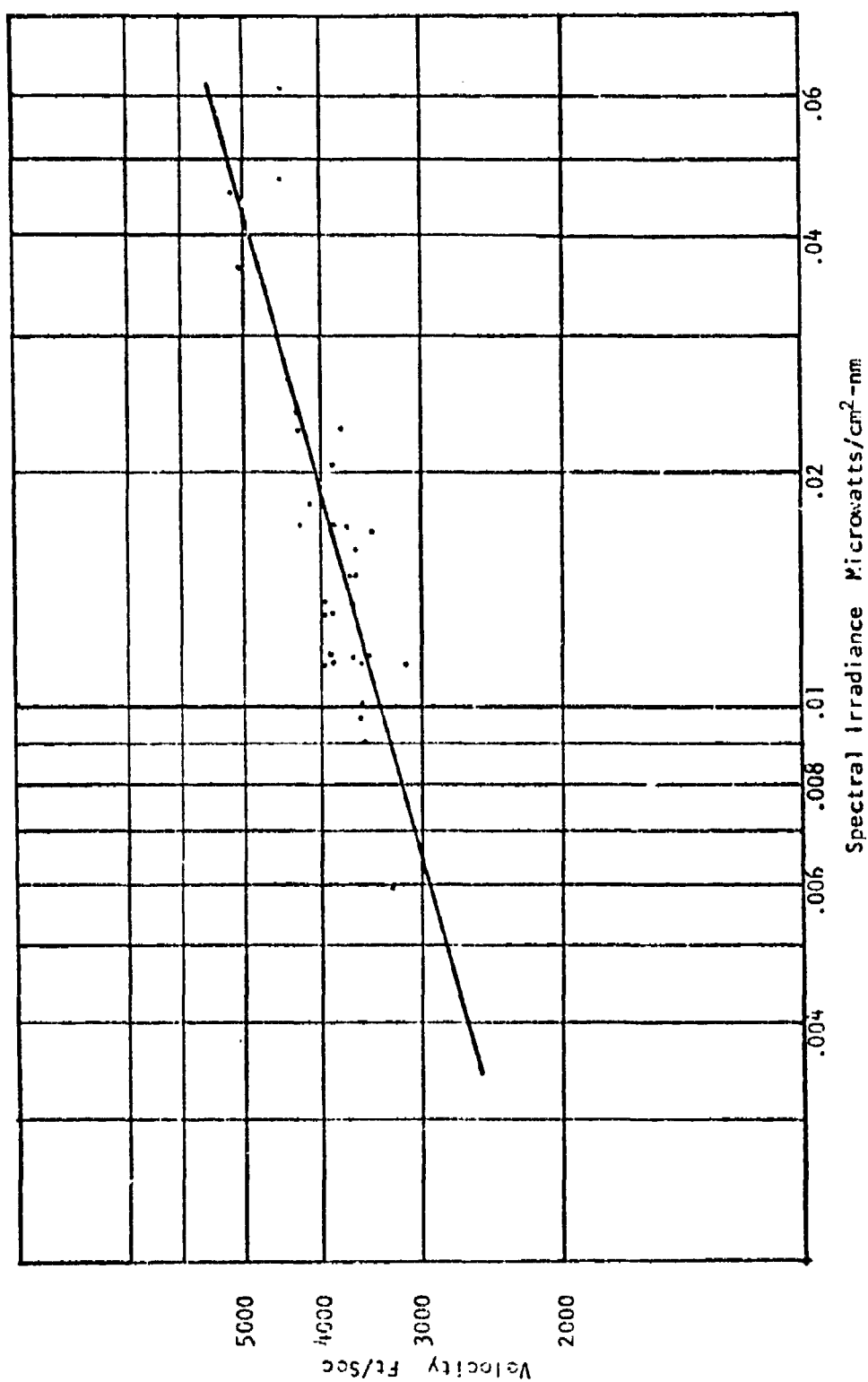
Figure 5. 4008A° Second Spectral Irradiance Maximum vs Velocity for 0.500 inch Sphere
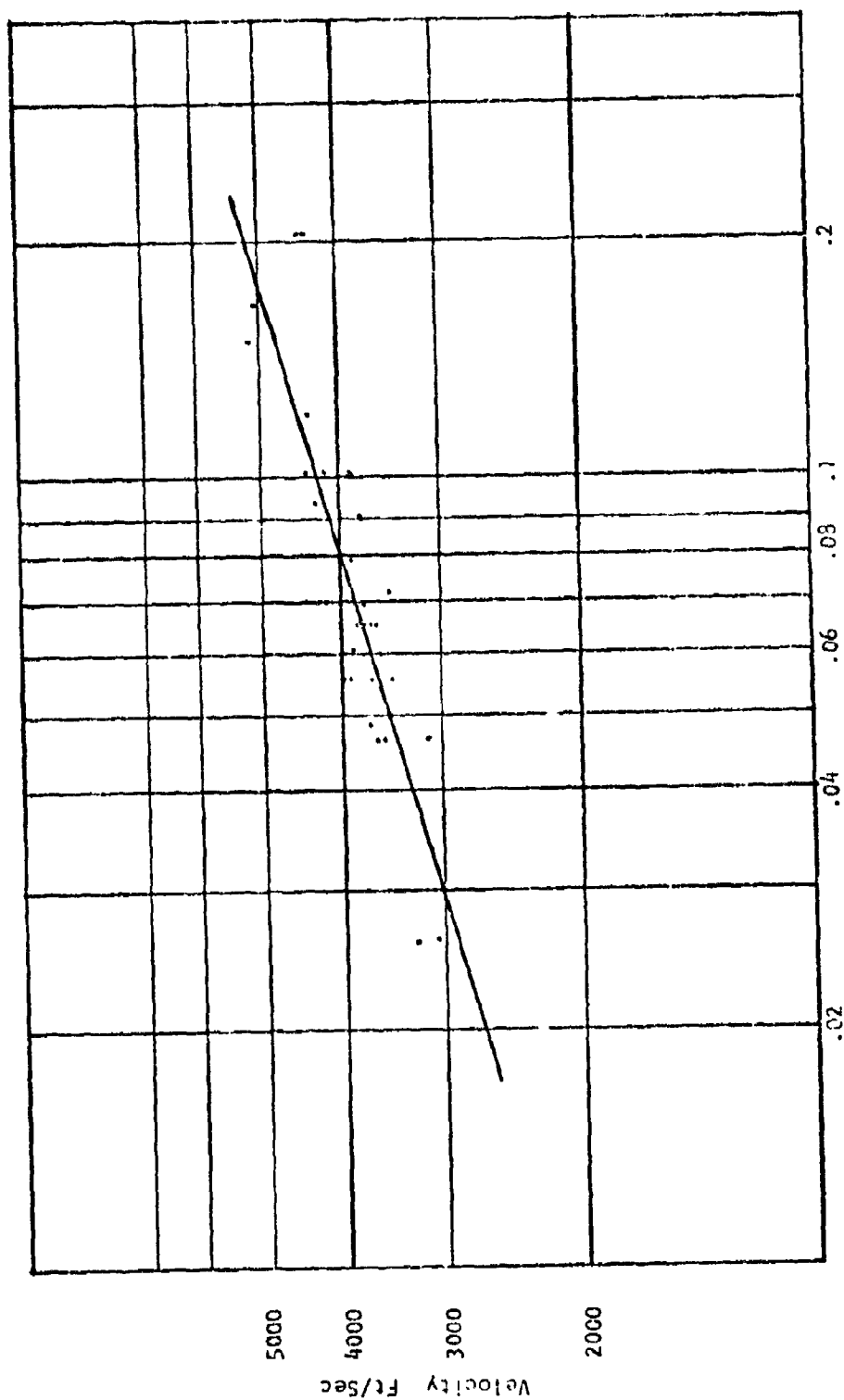
Figure 6.   7010A° Second Spectral Irradiance Maximum vs Velocity for 0.500 inch
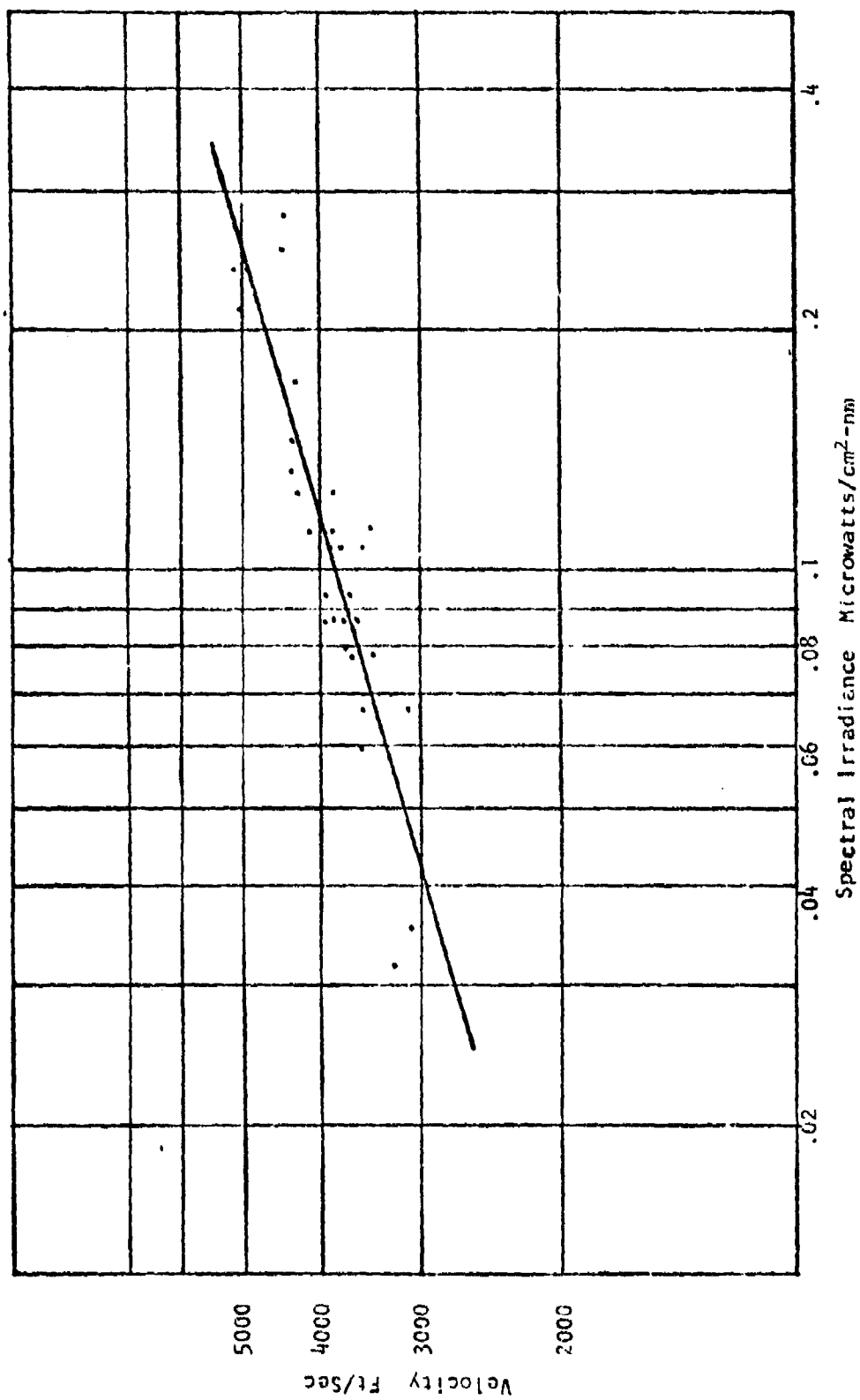Sphere

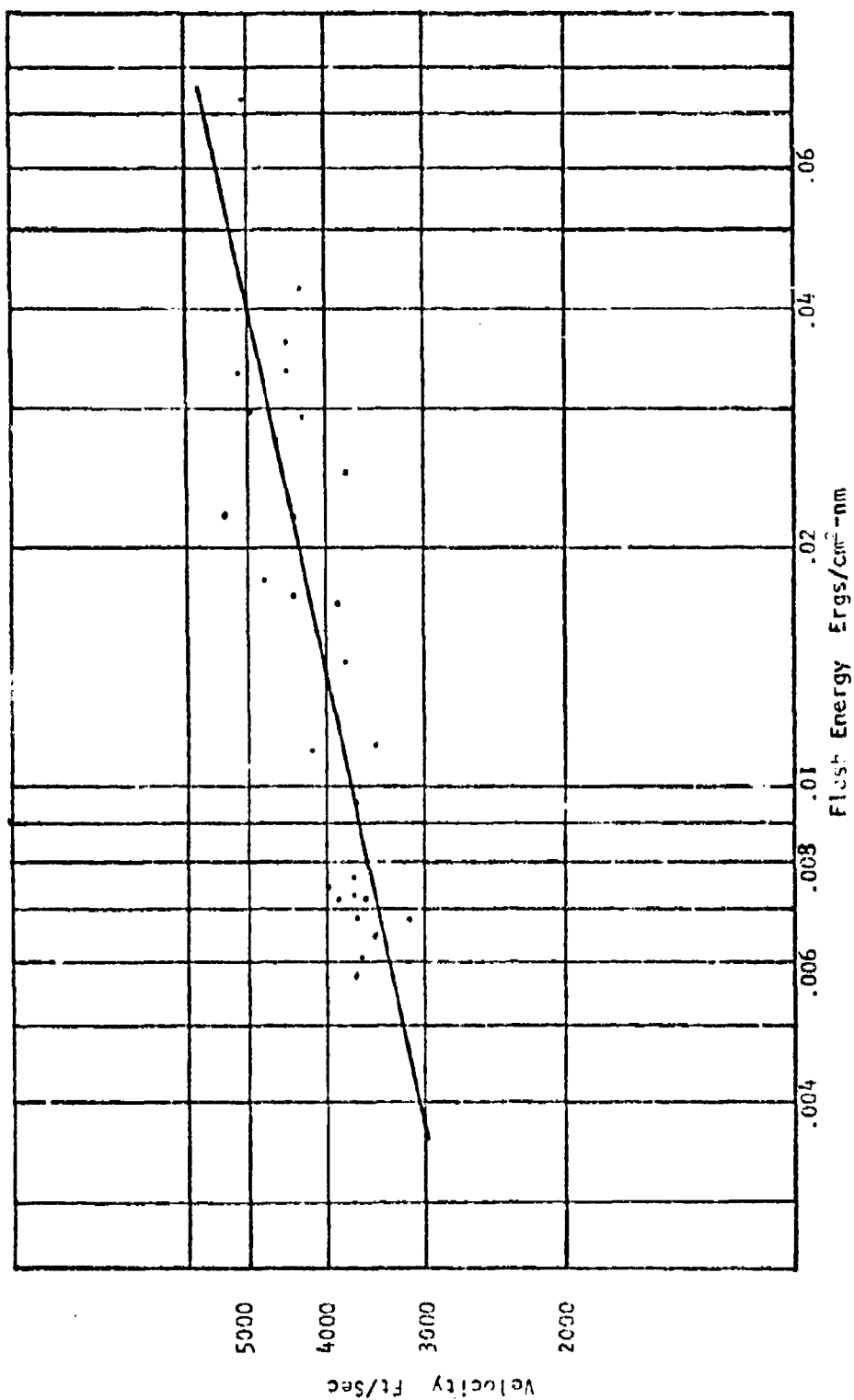Figure 7. 9025Å Second Spectral Irradiance Maximum vs Velocity for 0.500 inch Sphere

23
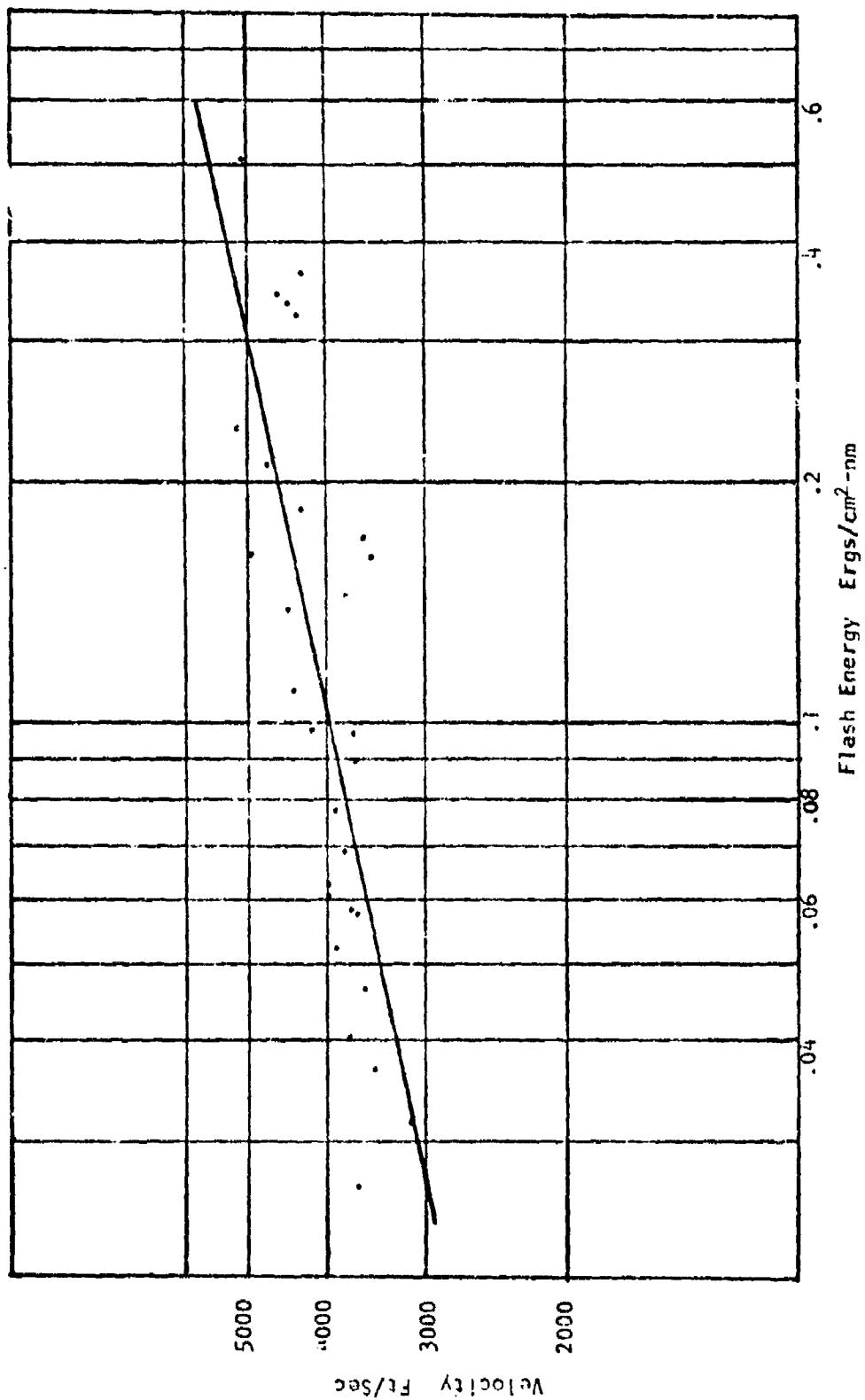
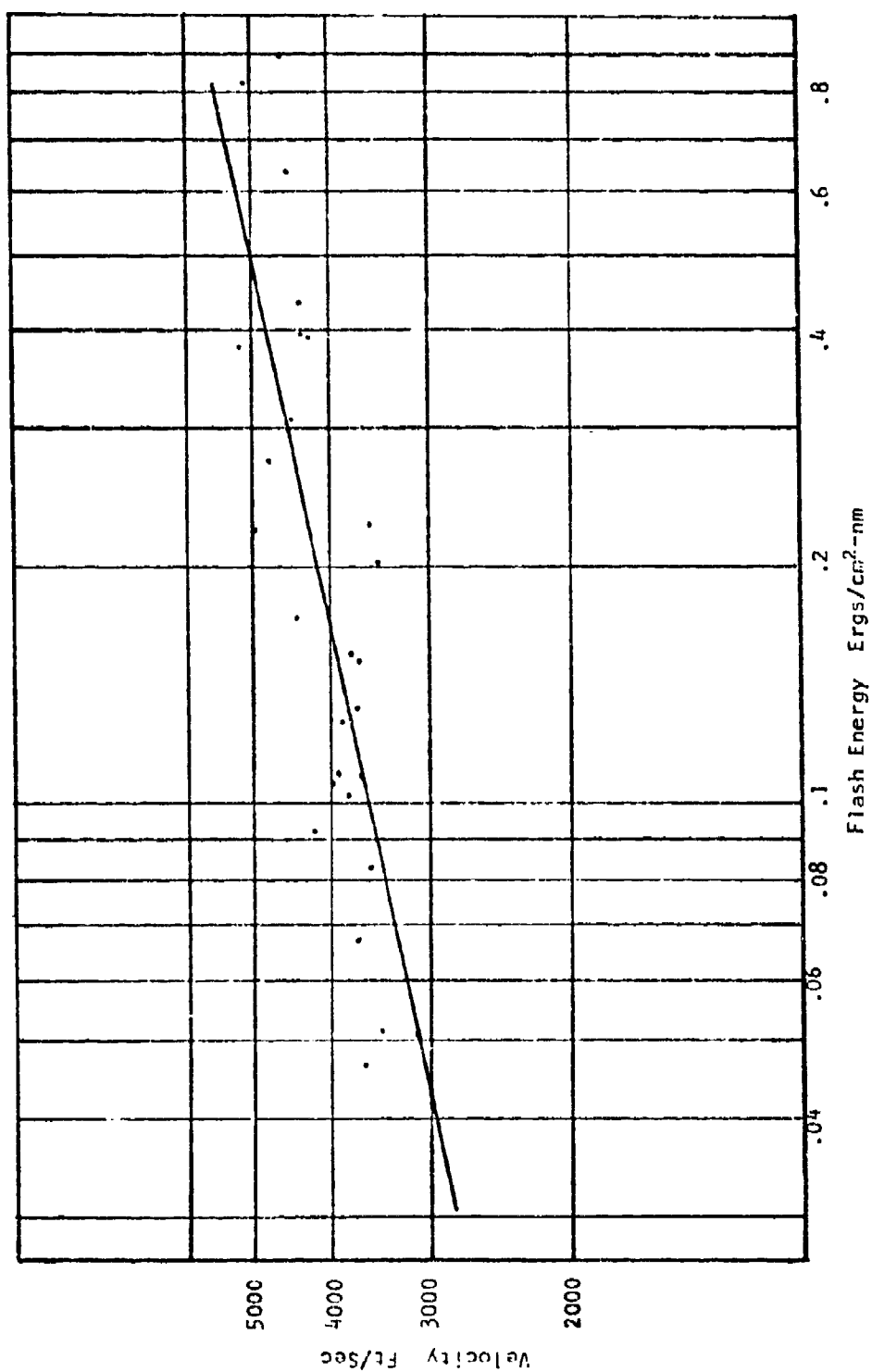Figure 8. 4008A° Flash Energy vs Velocity for 0.500 inch Sphere

Figure 9. 7010A° Flash Energy vs Velocity for 0.500 inch Sphere

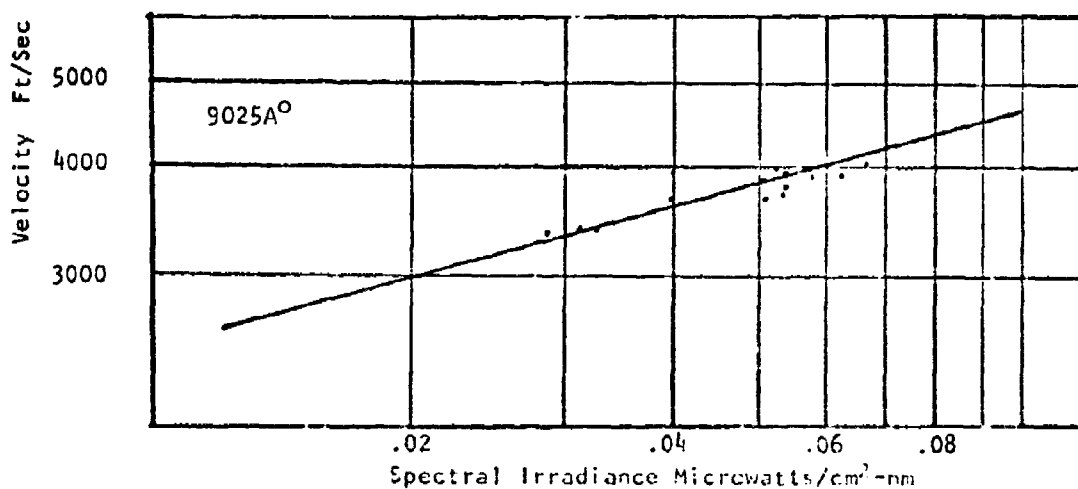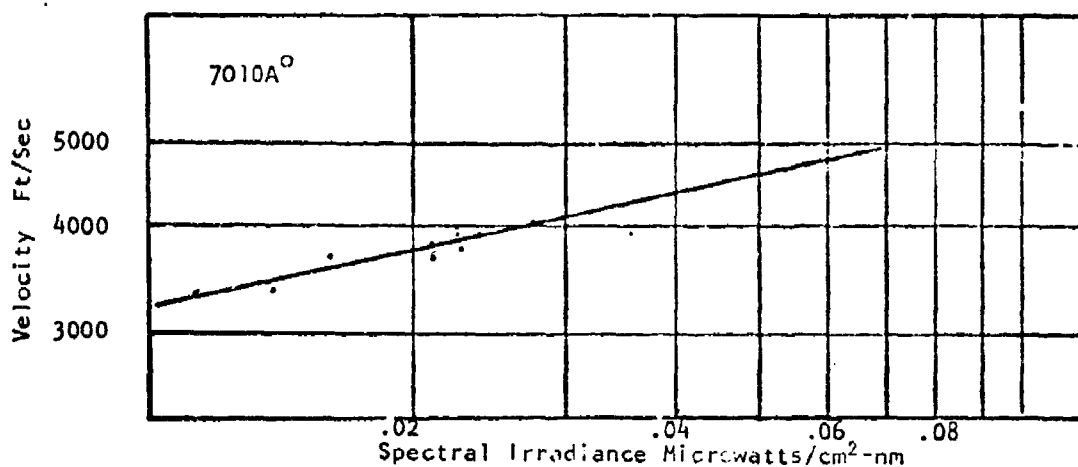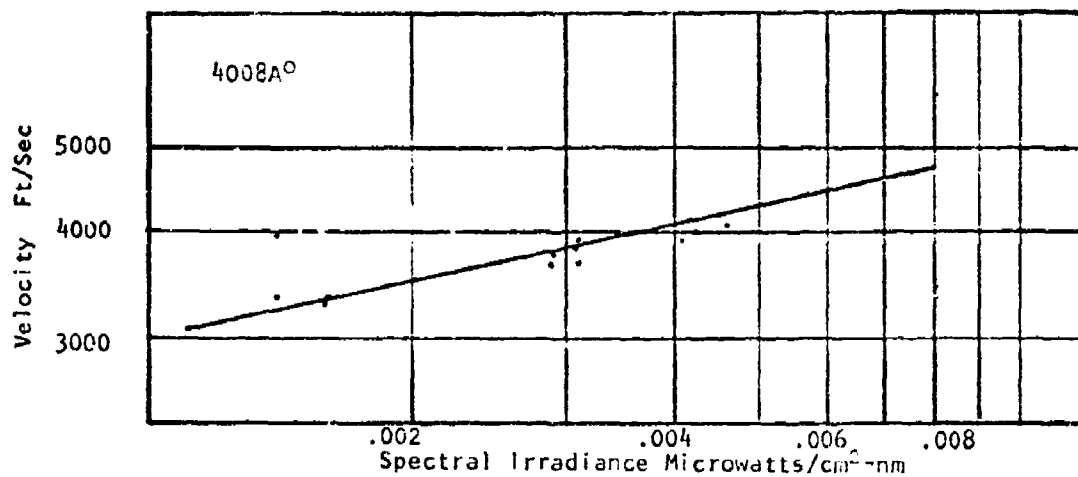Figure 10. 9025A° Flash Energy vs Velocity for 0.500 inch Sphere

Figure 11. First Spectral Irradiance Maximum vs Velocity for 0.343 inch Spheres

where X is the flash output in microwatts/cm^2-nm for the spectral

irradiance values and in ergs/cm^2-nm for the energy values; K is a

scaling constant; V is velocity in ft/sec; and n is slope of the line.

The equations of these lines are summarized in Table IV. Several impor-

tant facts can be observed from these plots and from Table IV.

Table IV

Flash Scaling Equations From Least Squares Curve Fit
of Experimental Data

0.500 Inch Sphere   <u>First Flash Maxima</u>

    4008A$^\circ$ $X = 1.922 \times 10^{-17} V^{4.65}$ μω/cm^2-nm

    7010A$^\circ$ $X = 6.37 \times 10^{-13} V^{3.88}$ μω/cm^2-nm

    9025A$^\circ$ $X = 6.59 \times 10^{-13} V^{3.67}$ μω/cm^2-nm

0.500 Inch Sphere   <u>Second Flash Maxima</u>

    4008A$^\circ$ $X = 5.97 \times 10^{-14} V^{3.75}$ μω/cm^2-nm

    7010A$^\circ$ $X = 1.97 \times 10^{-12} V^{3.50}$ μω/cm^2-nm

    9025A$^\circ$ $X = 2.86 \times 10^{-12} V^{3.52}$ μω/cm^2-nm

0.500 Inch Sphere   <u>Flash Energy</u>

    4008A$^\circ$ $X = 2.80 \times 10^{-18} V^{4.64}$ Ergs/cm^2-nm

    7010A$^\circ$ $X = 1.02 \times 10^{-17} V^{4.73}$ Ergs/cm^2-nm

    9025A$^\circ$ $X = 7.40 \times 10^{-18} V^{4.82}$ Ergs/cm^2-nm

0.343 Inch Sphere   <u>First Flash Maxima</u>

    4008A$^\circ$ $X = 2.01 \times 10^{-18} V^{4.79}$ μω/cm^2-nm

                                       $X = 4.79 \times 10^{-16} V^{4.37}$ μω/cm^2-nm

                                       $X = 6.38 \times 10^{-13} V^{3.60}$ μω/cm^2-nm

From the plots, spectral irradiance and energy values for a given pro-

jectile increase with increasing wavelength indicating that the higher

energy realm is probably in the IR range. From Table IV, the value of

n is approximately four for all equations, indicating that the spectral irradiance and energy for a given projectile scales as approximately the fourth power of the velocity.

One of the objectives of this study was to determine if a direct relationship exists between the impact flash and the energy or momentum of the projectile. Since the flash scales as the fourth power of projective velocity, the flash would have to scale as energy squared in order to be a function of energy only. That is, since

$$KE = \frac{1}{2} mV^2 \tag{12}$$

where KE is the projectile kenetic energy, and m is the projectile mass. To obtain a V^4 term, flash would have to depend on the square of the energy, as in m^2V^4.

Similarly, since

$$M = mV \tag{13}$$

where M is projectile momentum, the flash would have to depend on the fourth power of momentum in order to give a V^4 term, i.e., the flash would be proportional to m^4V^4. A comparison of the flash resulting from projectiles with different masses impacting at the same velocity should reveal the dependence on mass and whether or not either of those relationships exist. Comparing X_1 to X_2 gives

$$\frac{X_1}{X_2} = \frac{K_1 V^{N_1}}{K_2 V^{N_2}} = \frac{K_1}{K_2} V^{N_1 - N_2} , \tag{14}$$

But if the flash depends only on the energy the ratio should be

$$\frac{X_1}{X_2} = \frac{m_1^2 V^4}{m_2^2 V^4} = \frac{m_1^2}{m_2^2} \tag{15}$$

29

If cne flash depends only on the momentum the ratio should be

$$\frac{X_1}{X_2} = \frac{m_1^4 V^4}{m_2^4 V^4} = \frac{m_1^4}{m_2^4} \tag{16}$$

From Table IV, for $\lambda = 4008A^o$

$$\frac{X_{0.500}}{X_{0.343}} = \frac{1.922 \times 10^{-17} V^{4.65}}{2.01 \times 10^{-18} V^{4.79}} = 9.57 V^{.14} \tag{17}$$

Similarly for $\lambda = 7010A^o$

$$\frac{X_{0.500}}{X_{0.343}} = 1.33 \times 10^{-.49} \tag{18}$$

and for $\lambda = 9025A^o$

$$\frac{X_{0.500}}{X_{0.343}} = 1.03 V^{.07} \tag{19}$$

Table V shows values of those comparisons for various velocities.

Table V

Ratio of First Flash Spectral Irradiance for 0.500 Inch Spheres
to 0.343 Inch Spheres,
$I_{0.500}/I_{0.343}$

	3000 fps	4000 fps	5C00 fps
4008A^o	3.13	3.00	2.93
7010A^o	2.59	2.25	2.01
9025A^o	1.80	1.85	1.86

The projectile mass ratio is

$$\frac{m_{0.500}}{m_{0.343}} = \frac{129.5 \text{ grains}}{42.5 \text{ grains}} = 3.05 \tag{20}$$

The projectile frontal area ratio

$$\frac{A_{0.500}}{A_{0.343}} = \frac{.196 \text{ in}^2}{.0928 \text{ in}^2} = 2.11 \tag{21}$$

If the flash scaled as energy, the value of $X_{0.500}$ / $X_{0.343}$ would be expected to be $(m_{0.500}$ / $m_{0.343})$ or about 9, and if it scaled as momentum, the value of $X_{0.500}$ / $X_{0.343}$ would be expected to be $(m_{0.500}$ / $m_{0.343})^4$ or about 90. Table V shows that this is not the case. The flash resulting from different sized projectiles appears to scale as some more complicated function, possibly including energy, momentum, and size.

The theory of ablation and burning as the cause of the second flash intensity maximum is supported by the overall flash photograph shown in Figure 12.
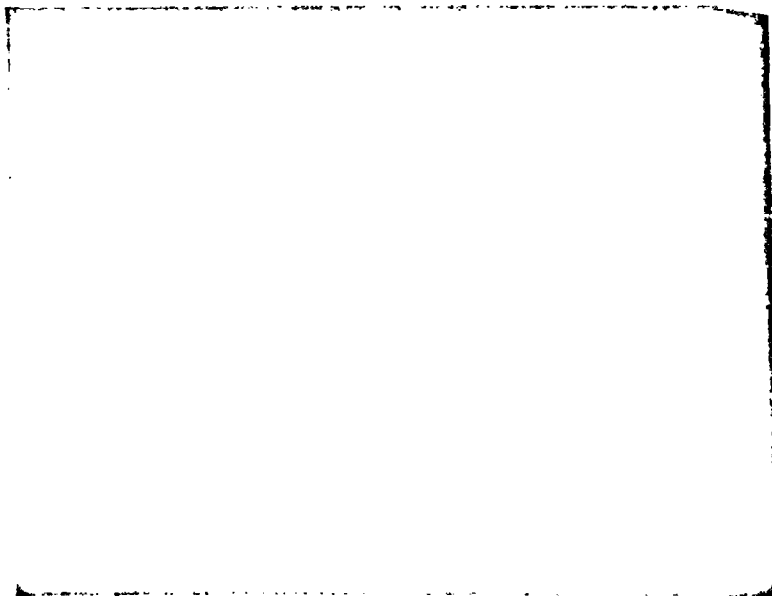

Figure 12. Still Photograph of Flash Resulting from Impact of 0.500 inch Sphere at 3860 fps

31

Several small particles can be seen to begin luminessing several inches downstream of the flash. This would correspond to the instant that enough thermal energy was gained to raise the particle to a temperature that would induce the burning phase of the flash model. This portion of the flash would be directly affected by changes in atmospheric pressure or composition.

An attempt was made to verify Kahler's (Ref 12) report that coating the target impact face reduced the flash. The upstream or impact side of several target sheets were coated with a .002 inch layer of aircraft fuel cell sealant. Some other targets were coated with epoxy based aircraft paint.

Due to range constraints, not enough shots were made to give conclusive quantitative results; however, both materials significantly reduced the downstream flash.

Table VI

Spectral Irradiance for First Flash Maximum
for Sealant Coated Targets. 0.500 inch Projectile

| Velocity | Spectral Irradiance-Microwatts/cm^2-nm | | |
	$4008A^o$	$7010A^o$	$9025A^o$
3991 fps	.000239	.0020	.00459
4372 fps	.0000725	.00573	.0133
4385 fps	.0000492	.00492	----
4386 fps	.000147	.013	.0212

32

Table VII

Spectral Irradiance for First Flash Maximum
for Epoxy Paint Coated Targets. 0.500 inch Projectile

| Velocity | Spectral Irradiance Microwatts/cm^2-nm | | |
	4008A$^{\circ}$	7010°	9025A$^{\circ}$
3643 fps	.0000875	.0018	.00529
3811 fps	.000275	.00317	.00846
3836 fps	.000172	.00408	.00846
4237 fps	.00016	.0171	.0296
4334 fps	.000122	.0146	.0310

Comparison of the values shown in Table VI with Figures 2 through 4 shows the effect of the sealant type coating to be

at 4008A$^{\circ}$ first flash maximum reduced by factors of

50 to 300

at 7010A$^{\circ}$ first flash maximum reduced by factors of

6 to 30

at 9025A   ash maximum reduced by factors of

8 to 25.

Similarly, comparison of Table VII with Figures 2 through 4 shows the effect of the epoxy paint coating to be

at 4008A$^{\circ}$ first flash maximum reduced by factors of

50 to 140

at 7010A$^{\circ}$ first flash maximum reduced by factors of

5 to 20

33

at 9025A° first flash maximum reduced by factors
of 5 to 20.

Second flash maximum data and total energy data were too small to
measure from the photomultiplier trace but appeared to be reduced by a
similar amount.

A few shots were fired into targets where the rear face was coated.
No quantitative data was obtained, however the effect appeared to be
considerably less than coating the front surface.

An abbreviated blackbody analysis was accomplished in an attempt to
determine if the flash radiated as a blackbody. If a light source
radiates as a blackbody, it should be possible to determine the temper-
ature of the source from the Planck equation

$$J_\lambda = C_1 \lambda^{-5} \Big/ (\text{EXP} \ (C_2/\lambda T) - 1) \tag{22}$$

where J_λ = the spectral irradiance in watts/cm^2-A° or similar units, C_1
and C_2 are constants, λ is wavelength and T is the temperature of the
source. Calculations of J_λ can be found in tabular form in Ref 21:82
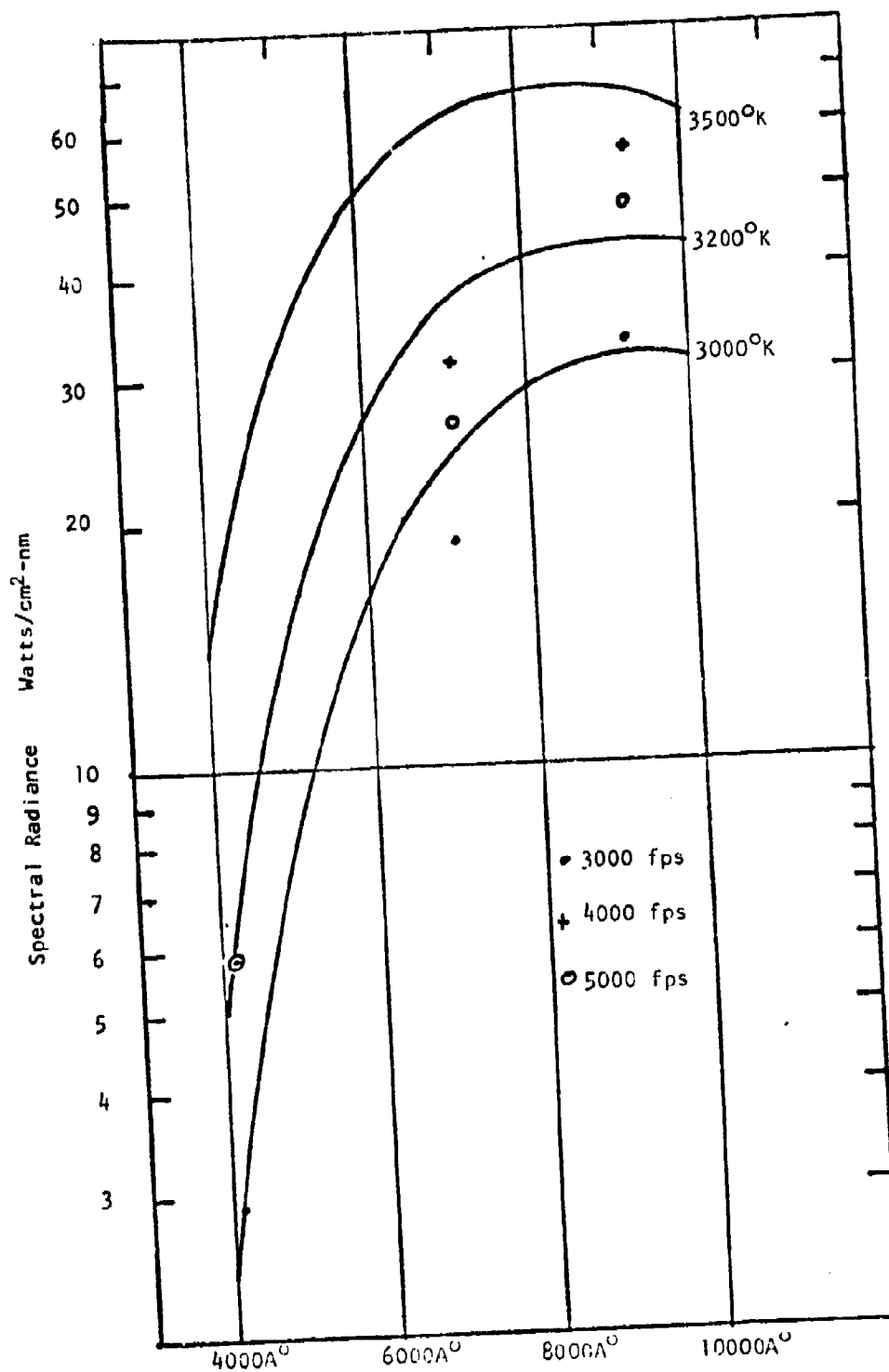and are plotted in Figure 13 as solid lines.

Figure 13. Comparison of Blackbody Temperature Curves with First Spectral Irradiance Maximum Values

35

To determine if the flash radiates as a blackbody, the values of spectral irradiance for the three different wavelengths for projectiles at various velocities (from Figures 2 through 4) were plotted to the same scale as Figure 13. The size and location of a blackbody introduces only a geometric constant term into the blackbody radiation values, J_λ. That is, the J_λ value in watts/cm^2-nm is actually

$$J_\lambda = \text{(source radiance)(source area)(solid angle}$$
$$\text{subtended by sensor)} \tag{23}$$

where the solid angle $= 4\pi r^2/R^2$
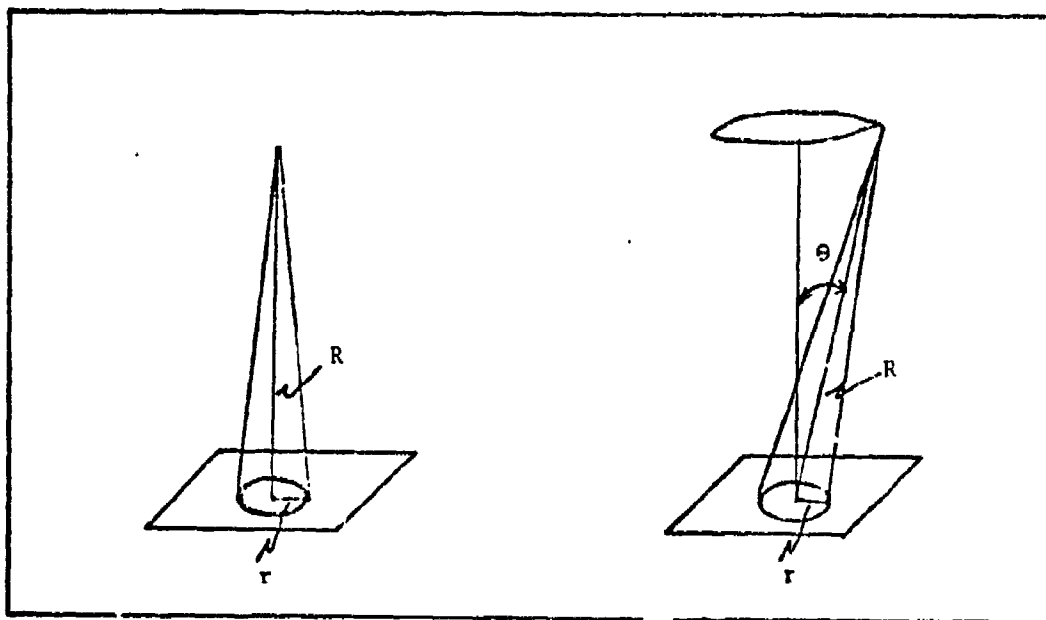
and r and R are depicted in Figure 14.

Figure 14.   Depiction of Blackbody Geometric
Constant

For a point on a finite source, the equation becomes

36

$$J_\lambda = \text{source radiance} \times \text{source area} \times \frac{4\pi(r\cos\ \iota)^2}{R^2} \qquad (24)$$

and as the area increases, θ increases, so the solid angle will change.
These changes in source area and solid angle result in a multiplicative
geometric constant. Since the vertical scale in Figure 13 is logarith-
mic, the experimental results can be translated along a vertical line
(at constant wavelength) to see if they match a blackbody temperature
curve. The values for the first spectral irradiance maximum for the
0.500 inch projectile are plotted as the points in Figure 13. The
experimental data did agree fairly well with the blackbody curves,
indicating that the flash does radiate as a blackbody. The temperature
of the flash, indicated by the temperature lines matched by the
experimental data, increases with increasing projectile velocity, from
3000°K at 3000 fps to 3200°K at 4000 fps and 5000 fps. This is close to
the value of 3400°K to 4100°K reported by Abernathy in Reference 1. The
impact flash was approximately 14 inches long and 5 to 7 inches in
diameter. Since the sensor, though painted at the center of the flash,
was only 60 inches away, some change in the geometric constant would be
expected as the flash size changed. This was the case, since the
geometric constant changed with changing projectile velocity.

V. Conclusions

The flash generated downstream of a target impacted by a high
velocity projectile is characterized by two intensity maximums. The
first occurs simultaneously or nearly simultaneously with the projectile
emerging from the target. The second occurs 30 to 80 microseconds later.
For a given projectile, the intensity maximums and the total flash energy
scale approximately as the fourth power of the projectile velocity.
The flash radiates as a blackbody at a temperature of about 3000°K at
3000 fps increasing to approximately 3200°K as velocity increases to
4000 fps and 5000 fps. The increase in the flash irradiance and energy
as the fourth power of velocity together with the increase in flash
temperature with velocity makes hyper-velocity shrapnel from sources
such as surface-to-air missiles an important kill mechanism. Coating
the upstream side of the target with epoxy paint or fuel cell sealant
material reduces the downstream flash by factors of 5 to 300, depend-
ing on wavelength examined. This phenomena needs much more
investigation to determine its cause and to develop a flash suppressant
material effective against higher velocity impacts.

VI. Recommendations

The analysis of this investigation has led to several recommendations.

1. A further study be undertaken using various sized projectiles to determine the relationship between flash and size and/or mass.

2. A further study be undertaken using various shaped projectiles having a constant mass to determine the relationship between flash and projectile shape.

3. A further study be undertaken to determine the cause of the reduction in impact flash obtained by coating the target.

4. Using information obtained in recommendation 3, an intensive search should be made for an effective flash suppressant substance suitable for use in aircraft and/or aircraft component paint.

Bibliography

1. Abernathy, J. B. Ballistic Impact Flash. GAW/MC/68-1. Air Force Institute of Technology, Wright-Patterson Air Force Base, Ohio, 1968.

2. Altshuler, L. V., et. al., "Equation of State for Aluminum and Lead in the High Pressure Region". Soviet Physics JETP, 11:573, 1960.

3. Backman, M. E. and W. J. Stronge. Penetration Mechanics and Past Perforation Effects in an Aluminum-Aluminum Impact System, NWC P4414, China Lake, California, 1967.

4. Boice, R. T., Jr. Synergistic Damage Caused by Multiple Fragment Impact on Closed Systems. GAW/MC/74-10. Air Force Institute of Technology, Wright-Patterson Air Force Base, Ohio, 1974.

5. Brockert, P. E. and W. C. Cooley, Development of an Impact Flash Spectrometer. Project No. 7844, Directorate of Armament Development, Eglin Air Force Base, Florida, 1965.

6. Caron, A. P. Oxidative Detonations Initiated by High Velocity Impacts. Air Force Flight Dynamics Laboratory, TR 65-41, Wright-Patterson Air Force Base, Ohio, 1965.

7. Deal, W. E., "Shock Hugoniat of Air", Journal of Applied Physics 28:782-784, 1957.

8. Dunn, D. J. Some Measurements of the Time Delay Between Fragment Impact and Target Flash. BRL-MR-517, Ballistic Research Laboratory, Aberdeen Proving Ground, Maryland, 1950.

9. Friend, W. H., et. al., An Investigation of Explosive Oxidations Initiated by Hyper-Velocity Impacts. AFFDL-TR-67-92, Wright-Patterson Air Force Base, Ohio, May 1967.

10. Friichtenicht, J. F. Experiments on the Impact-Light-Flash at High Velocities. NASA CR-416, Washington, D. C., 1966.

11. Jean, B. and T. L. Rollins. Hypervelocity Impact Flash for Hit Detection and Damage Assessment. AFATL TR-68-46, Eglin Air Force Base, Florida, 1968.

12. Kahler, R. L. Impact Flash Suppression. Joint USAF-USN Technical Symposium on Aircraft and Missile Vulnerability. Wright-Patterson Air Force Base, Ohio, 1952.

13. Keough, D. D. Luminosity Studies of High Velocity Impact. AFCRL TR-60-415, Bedford, Massachusetts, 1960.

14. Kottenstette, J. P. and E. Wittrock. Impa_ Flash Characteristics as Affected by Oxidixing Materials. AFATL-TR-67-2, Eglin Air Force Base, Florida, 1967.

15. Kraft, J. M., "Surface Friction in Ballistic Penetration". Journal of Applied Physics 26:1248-1252, 1955.

16. McQueen, R. C. and S. P. Marsh, "Equation of State for Nineteen Metallic Elements from Shock Wave Measurements to Two Megabars". Journal of Applied Physics 31:1253, 1960.

17. National Bureau of Standards. Report of Calibration of One Standard of Spectral Irradiance, Report No. 185839, Washington, D.C., 1965.

18. Phototubes and Photocells, Technical Manual PT-60, Radio Corporation of America, Lancaster, Pennsylvania, 1963.

19. Recht, R. F., "Catastrophic Thermoplastic Shear". Journal of Applied Mechanics, 31:189-193, 1964.

20. Rice, M. H., et. al., "Compression of Solids by Strong Shock Waves". Solid State Physics, Vol 6, edited by F. Seitz and D. Turnbull. Academic Press, Inc., New York, New York, 1958.

21. Smithsonian Physical Tables (Ninth Revised Edition), Smithsonian Institution. Washington, D. C., 1954.

22. Thompson, W. T. "An Approximate Theory of Armour Penetration", Journal of Applied Physics, 26:80, 1955.

23. Tucker, P. E., et. al., The Relationship Between Luminosity and Ionization in the Trails of High Velocity Pellets. Department of Electrical Engineering, University of Utah, Salt Lake City, Utah, 1957.

24. Zel'Dovich, Ya. B. and Yu. P. Raizer. Physics of Shock Waves and High Temperature Hydrodynamic Phenomena. Chapter 11. Translated by J. F. Heyda. General Electric Company, Space Science Laboratory, King of Prussia, Pennsylvania.

APPENDIX A

Description of Equipment

The experimental portion of this investigation was accomplished in Building 57, Area B, Wright-Patterson Air Force Base, Ohio. This facility was temporarily converted to an indoor gun range. The overall apparatus set up is described in Figure 15.
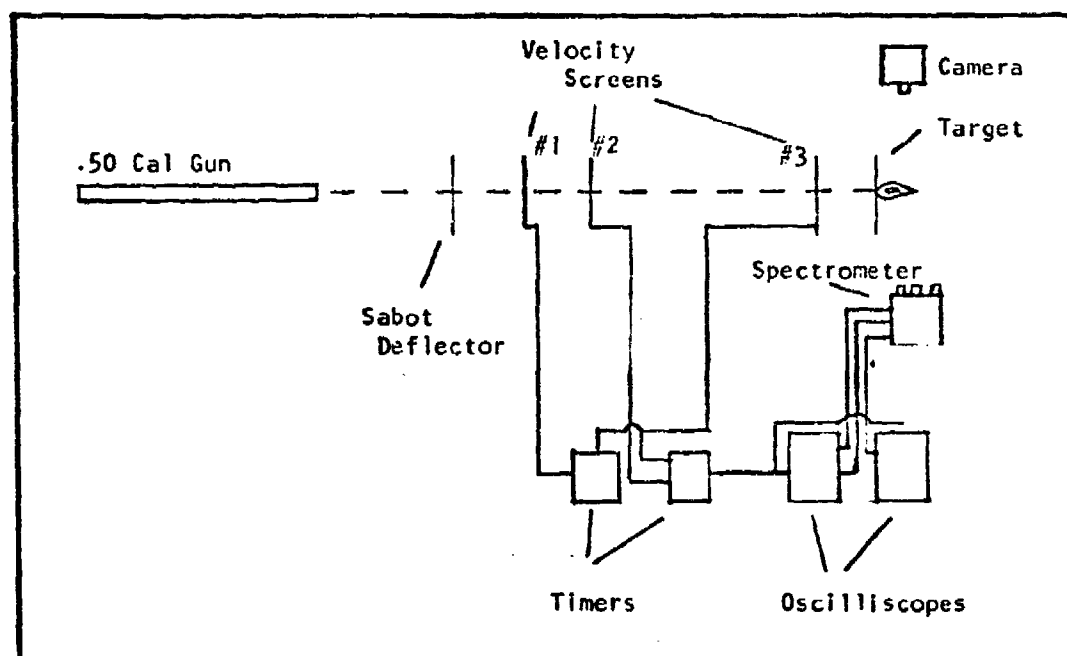

Figure 15. Apparatus Set Up

1. .50 Caliber Smooth Bore Gun. The Air Force Flight Dynamics Laboratory furnished a .50 caliber smooth bore gun chambered to accept a standard military casing. The gun is fired by an electrically operated solenoid. By varying powder loads from 80 grains to the

maximum cartridge capacity of 205 grains of Dupont 2400 powder, projectile velocities ranging from 2100 fps to 4400 fps were obtained. To increase the projectile velocity above this level, the air was evacuated from the gun barrel by sealing the end of the barrel with a piece of paper, and attaching a vacuum line to a port in the side of the barrel. The pressure inside the barrel was thereby reduced to 15 mm Hg. This procedure increased projectile velocity by slightly over 10% for the same powder loads.

2. Instrumentation

Velocity Measurement. The velocity was measured over a 26 foot distance, 2 foot prior to the target plate. Three velocity screens consisting of continuous line printed circuit paper were used. When the projectile passed through the first screen, one Hewlett-Packard Model 5300A Timer was started, four foot later the projectile passed through the second screen, starting a second identical timer, then 22 foot later it passed through the third screen, which stopped both timers. The timer read-outs were in microseconds, providing data to calculate velocities to the nearest foot per second. The velocities used in this paper are an average of these two values.

Impact Flash Spectrometer. This system consists of an Exotech three channel spectrometer, power supply console, and two Tectronix 555 dual beam oscilloscopes. The spectrometer assembly consists of three photomultiplier tubes and associated circuitry, as well as narrow band by-pass filters and neutral density filters. A photomultiplier tube consists of a photocathode, a secondary emission multiplier, and an anode. Photons from the light source strike the

43

photocathode. This release a number of electrons, which are accelerated onto the first stage or dynode of the multiplier, where they each release additional secondary electrons, which are accelerated onto the next dynode, and so on. A potential gradient is maintained between the successive dynode stages. The electrons released by the last dynode are collected at the anode, which releases an electric pulse as the tube output. The photomultiplier tubes used in this unit are two S-20 type visible range tubes, and one S-1 infrared tube. Response curves for these photomultipliers are shown in Figure 16. All three have identical circuitry as shown in Figure 17. Narrow band by-pass filters were used to allow flash examination at various wavelengths. The spectral ranges of these filters are shown in Figure 18. To avoid saturating the photomultipliers, Kodak Wratten neutral density filters were used to reduce the number of photons striking the sensors. These filters were calibrated for each photomultiplier/narrow band by-pass filter combination. This data is presented in Appendix B. The electrical impulse from the photomultiplier tubes was routed to the two oscilloscopes. The scope sweeps were triggered by the third sheet of printed circuit paper in the velocity measurement apparatus. Experiments conducted using a signal generator providing impulses to a diode light source showed that the spectrometer system would follow a one microsecond duration light signal, provided by the tubes were not saturated by the intensity of the light.

Still Camera. A 4 x 5 speed graphic camera using Polaroid film was used to record an overall picture of the flash. The shutter was opened using a remote trigger just prior to the shot and closed immediately after the flash.
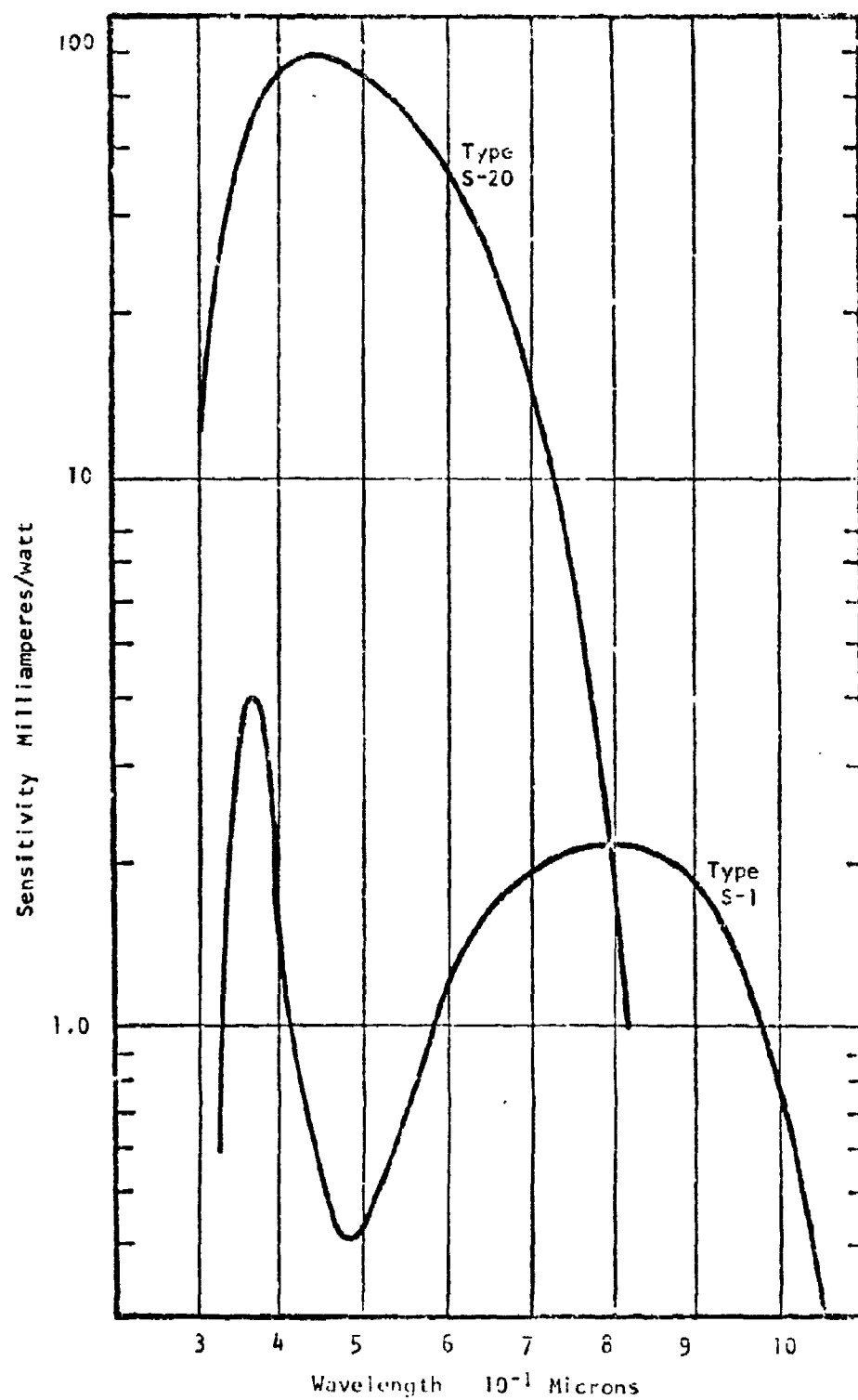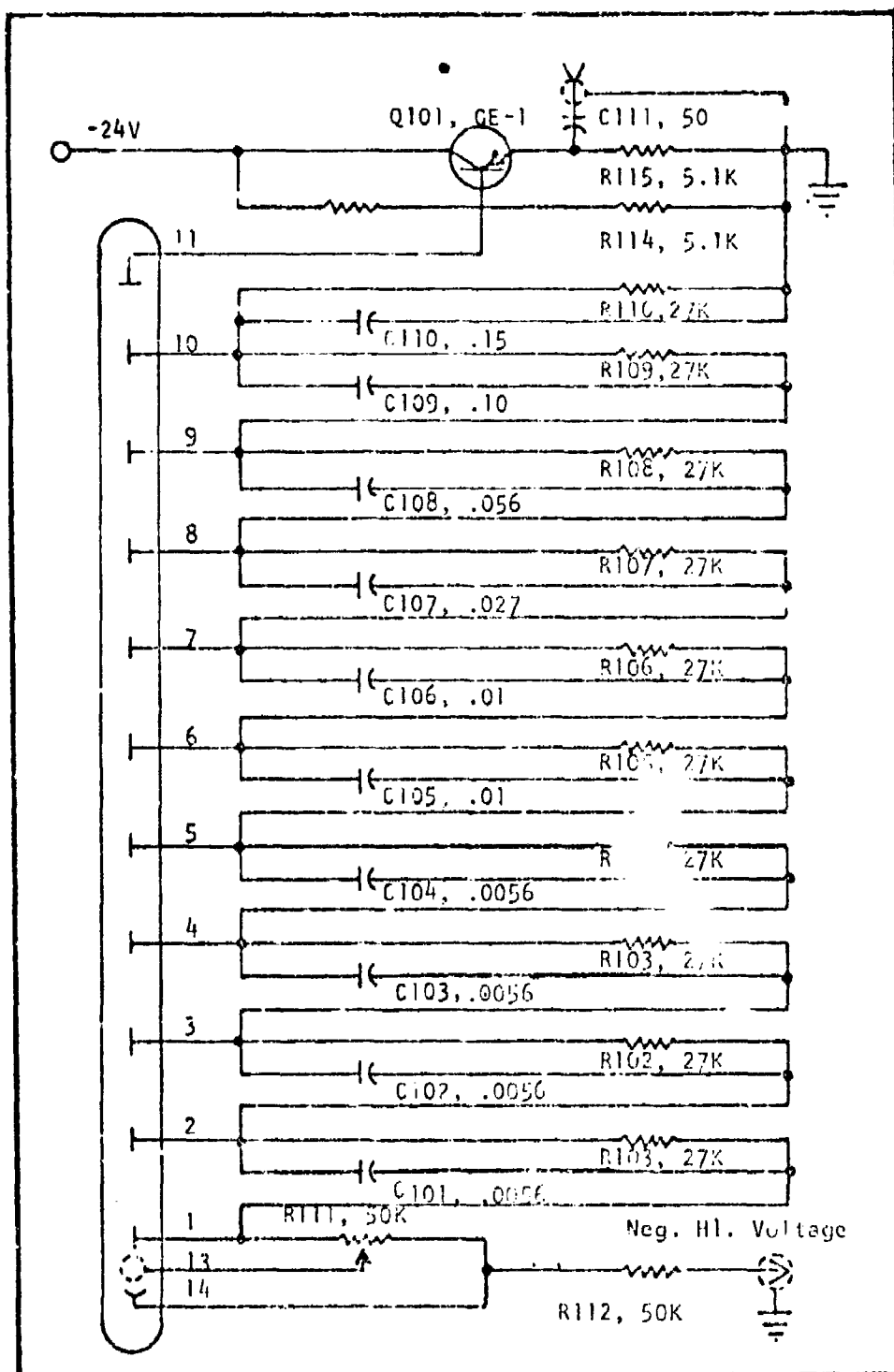
Figure 16. Photomultiplier Spectral Response

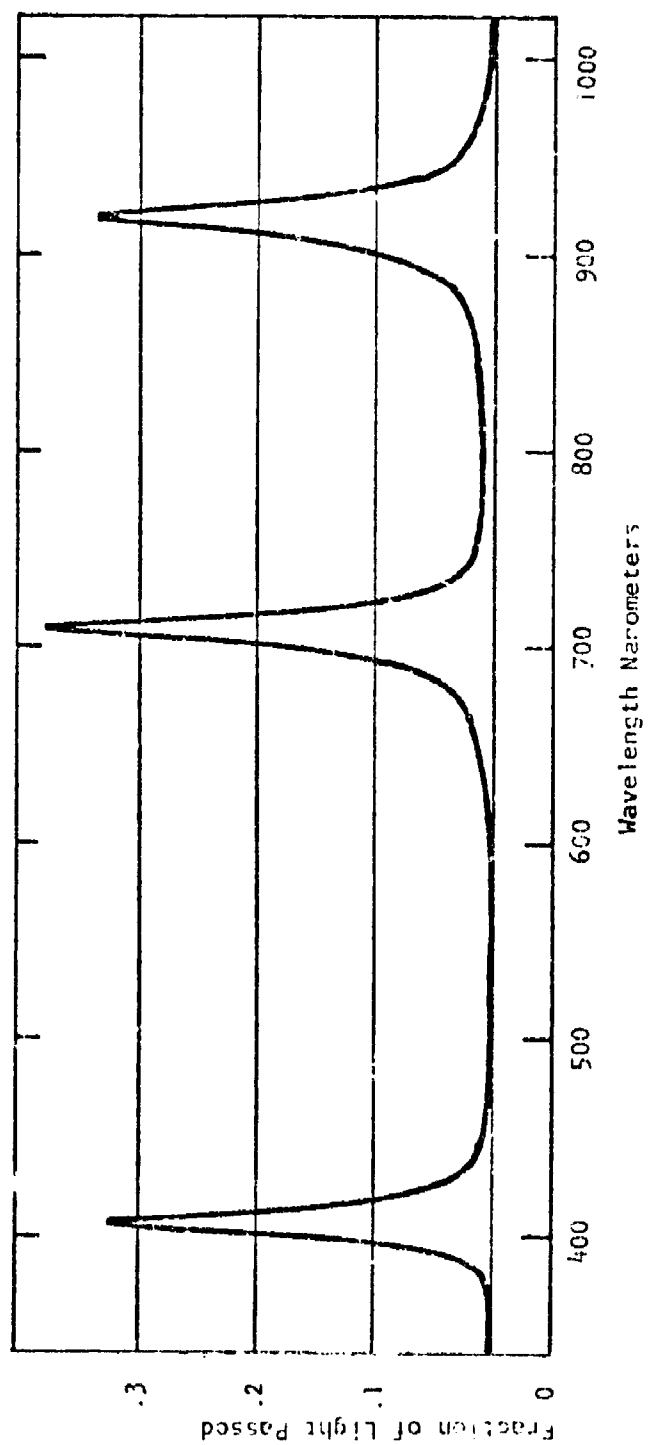Figure 17. Photomultiplier and Emitter Follower Circuitry

Figure 18. Spectral Response of Narrow Band By-Pass Filters

47

APPENDIX B

Calibration

1. Calibration of Photomultipliers

The calibration light source assembly consists of a 1000 watt quartz iodide bulb and a mechanical chopper. The bulb is housed in a 24 inch diameter, 36 inch high cylinder, with an aperture allowing a beam of light to pass through the chopper assembly. The chopper consists of an 18 inch diameter disc with a single slot. The disc is connected to a small motor which turns the disc at about 3000 rpm. The "chopped" light is then directed on to the spectrometer sensors for calibration. The chopper serves the purpose of modulating the signal to allow measurement of the difference between zero signal and known source signal. The light source was calibrated by the National Bureau of Standards (Ref 17) in microwatts per cm^2-nanometer at a distance from the source of 50 cm giving

For 4008°A	2.28 $\mu\omega/cm^2$-nm
7010°A	21.1 $\mu\omega/cm^2$-nm
9025 A	25.28 $\mu\omega/cm^2$-nm

Calibration Procedure. The spectrometer unit, with narrow band by-pass filters installed, was placed at various distances from the calibration light source. The scope output in volts was noted and recorded for each position. Since the light intensity should change by the square of the distance, a constant value of D^2V was expected, where V is the recorded voltage, and D is the distance between the source and the sensor. Values of D^2V constant within five percent were obtained. From this an average value of D^2V at the various wavelengths was

calculated,

$$4008\text{A}^\circ \qquad D^2V = 2313 \ ft^2 \ volt$$

$$7010\text{A}^\circ \qquad D^2V = 3090 \ ft^2 \ volt$$

$$9025\text{A}^\circ \qquad D^2V = 257.8 \ ft^2 \ volt$$

These values were then used to calculate the conversion factor necessary to convert the flash induced scope output to $\mu w/cm^2$-nm.

Sample Calculation of Conversion Factor. For λ = 4008A$^\circ$, at 50 cm - 1.64 ft, the source produces 2.28 $\mu w/cm^2$-nm. Since the D^2V constant for this wavelength is 2313 ft^2 volts, at a distance of 1.64 ft, an output of

$$\frac{2313}{1.64^2} \quad \frac{ft^2 \ volts}{ft^2} = 860 \ volts \tag{25}$$

would be expected as a result of 2.28 $\mu w/cm^2$-nm of light irradiance produced by the source. This gives for 1.65 ft,

$$\frac{2.28 \ \mu w/cm^2\text{-nm}}{860 \ volt} = \frac{.00265 \ \mu w/cm^2\text{-nm}}{volt} \tag{26}$$

at D = 5 foot, which is the distance from the flash to the sensors, the scale factor required to convert the scope reading from volts to microwatts/cm^2-nm is

$$Scale \ Factor \quad = \quad \frac{(.00265 \ \mu w/cm^2\text{-nm}/volt) \ (5.0^2 ft^2)}{1.64^2 ft^2} \tag{27}$$

$$= \quad .0246 \ \mu w/cm^2\text{-nm}/volt$$

Similarly at λ = 7010A$^\circ$

$$Scale \ Factor \quad = \quad .0102 \ \mu w/cm^2\text{-nm}/volt$$

and for λ = 9025°A

$$Scale \ Factor \quad = \quad .0706 \ \mu w/cm^2\text{-nm}/volt$$

49

2. Calibration of Kodak Wratten Neutral Density Filters

Kodak Wratten N. D. 96 filters rated at .1, .4, .5, .6, 1.0, and 2.0 were used. To determine the amount of light passed scope readings were taken with and without them. In addition, combinations of the different strength filters were used to insure the readings remained valid. The results of this are shown in Table VIII.

Table VIII

Amount of Light Passed at Selected Wavelengths
by Kodak Wratten N.D. 96 Filters

	Amount of Light Passed		
Filter No.	$4008A^\circ$	$7010A^\circ$	$9025A^\circ$
.4	.40	.4	a
.5	a	a	.282
.6	.206	.251	a
1.0	.066	.107	.268
2.0	.0054	a	a

a - Not Measured

VITA

John W. Mansur was born on 16 April 1940, in Grand Junction, Colorado. He attended the University of Colorado and graduated in 1963 with a Bachelor of Science Degree in Aeronautical Engineering. After being commissioned in the Air Force, he completed pilot training in 1964. He has had a varied flying career, including three assignments to SEA. He entered the Institute of Technology in 1972.

    Permanent address: in care of: Howard Brouse
                                            Whitewater, Colorado 81527